수의학 박사학위 논문

# Lace1 Deficiency Promotes Lactate-induced Beige Adipogenesis in Mouse Model

Lace1 유전자 결손마우스의
젖산 유도 베이지 지방 생성 연구

2022 년 8 월

서울대학교 대학원
수의학과 수의생명과학 전공
(수의발생유전학)
김 연 주

**A Dissertation for the Degree of Doctor of Philosophy**

# Lace1 Deficiency Promotes Lactate-induced Beige Adipogenesis in Mouse Model

August 2022

Youn Ju Kim

Supervisor: Prof. Je Kyung Seong, D.V.M., Ph.D.

Department of Veterinary Medicine
Veterinary Life Science
(Major: Veterinary Developmental and Genomics)

The Graduate School of Seoul National University

# Lace1 Deficiency Promotes Lactate-induced Beige Adipogenesis in Mouse Model

지도교수 성 제 경

이 논문을 수의학박사 학위논문으로 제출함

**2022 년 5 월**

서울대학교 대학원

수의학과 수의생명과학전공

김 연 주

김연주의 수의학박사 학위논문을 인준함

**2022 년 7 월**

위 원 장 윤 여 성 (인)

부위원장 성 제 경 (인)

위 원 오 승 현 (인)

위 원 이 윤 희 (인)

위 원 황 성 순 (인)

# ABSTRACT

# Lace1 Deficiency Promotes Lactate-induced Beige Adipogenesis in Mouse Model

By
**Youn Ju Kim**

Graduate School of Seoul National University

**Supervisor: Prof. Je Kyung Seong, D.V.M., Ph.D.**

Adipose tissue browning is essential for maintaining energy homeostasis against obesity. Recent studies have reported that lactate metabolites contribute to white adipose tissue (WAT) browning in a β3-AR stimulation-dependent manner. the mitochondrial ATPase gene, Lactation elevated 1 (Lace1) is a mitochondrial integral membrane protein that mediates mitochondrial protein homeostasis. However, its role in beige adipose tissue is unknown. In this study, I suggested that Lace1 mediates browning capacity in iWAT under CL-316,243 (CL) challenge, using lactate from heart.

To investigate Lace1 expression in beige fat, I injected mice with the beta3 adrenergic receptor (β3-ARs) agonist, CL, once a day for 3 days, and challenged the mice with cold exposure (4-6 °C) for 1 week. Also, mice were trained under voluntary wheel running aerobic exercise for 4 weeks. To identify the functions of Lace1 in brown and beige adipocytes, I used an immortalized brown pre-adipocyte (iBPA) cell line and primary iWAT cells from C57BL/6N mice. Additionally, I applied CL, cold, and exercise challenges to Lace1 null KO mice to confirm the browning capacity of iWAT, BAT and heart compared with wild-type (WT) mice. Lace1 increased during beige and brown adipogenesis and was more enriched in CL-, cold- and exercise-induced beige fat than in white fat. I found that Lace1 and Ucp1 (uncoupling protein 1) were positively correlated in iWAT under browning stimuli and confirmed that thermogenesis-related gene expression increased in Lace1 KO mice iWAT compared with WT mice, concomitant with increased energy expenditure under CL challenge and cold exposure. Notably, Lace1 deletion increased lactate uptake and browning of iWAT compared with control littermates under CL challenge. The enhanced browning ability using lactate in Lace1 KO mice was due to increased lactate release by pyruvate dehydrogenase inactivation in heart tissue.

Taken together, this study identified the role of Lace1 in mediating iWAT browning capacity by lactate release from heart.

**Keywords**: adipose tissue browning, iWAT browning, inguinal white adipose tissue, adipogenesis, Lace1, beige adipose tissue, thermogenesis, Ucp1, Uncoupling protein 1, cardiac hypertrophy, heart, lactate, pyruvate dehydrogenase

**Student number: 2015-21808**

# LIST OF ABBREVIATIONS

| | |
|---|---|
| **AA** | Antimycin A |
| **AFG1** | ATPase family gene 1 |
| **ATP** | Adenosine triphosphate |
| **BAT** | Brown adipose tissue |
| **βAR** | beta adrenergic receptor |
| **cAMP** | cyclic adenosine monophosphate |
| **CAS9** | CRISPR-associated protein 9 |
| **COX4** | Cytochrome c oxidase 4 |
| **CIDEA** | Cell death-inducing DNA fragmentation factor alpha-like effector A |
| **CL** | CL-316,243 |
| **CRISPR** | Clustered regularly interspaced short palindromic repeats |
| **DEGs** | Differentially expressed genes |
| **DMEM** | Dulbecco's modified eagle medium |
| **DNA** | Deoxyribonucleic acid |

| | |
|---|---|
| **ELISA** | Enzyme-linked immunosorbent assay |
| **eWAT** | Epididymal white adipose tissue |
| **FA** | Fatty acid |
| **FBS** | Fetal bovine serum |
| **FCCP** | Carbonyl cyanide-4(trifluoromethoxy) phenylhydrazone |
| **GAPDH** | Glyceraldehyde 3-phosphate dehydrogenase |
| **GEO** | Gene expression omnibus |
| **GO** | Gene ontology |
| **GPR81** | G-protein-coupled receptor 81 |
| **Hcar1** | Hydroxycarboxylic acid receptor 1 |
| **H&E** | Hematoxylin & Eosin |
| **HSL** | Hormone-sensitive lipase |
| **iBPA** | Immortalized brown pre-adipocytes |
| **IHC** | Immunohistochemistry |
| **iWAT** | Inguinal white adipose tissue |
| **KD** | Knock down |

| | |
|---|---|
| **KEGG** | Kyoto Encyclopedia of Genes and Genomes |
| **KO** | Knock out |
| **LACE1** | Lactation elevated 1 |
| **LDH** | Lactate dehydrogenase |
| **MCT** | Monocarboxylate transporter |
| **mRNA** | Messenger RNA |
| **NMR** | Nuclear magnetic resonance |
| **OCR** | Oxygen consumption rate |
| **PDH** | Pyruvate dehydrogenase |
| **PGC1α** | Peroxisome proliferator-activated receptor gamma coactivator 1-alpha |
| **PBS** | Phosphate-buffered saline |
| **PCR** | Polymerase chain reaction |
| **PKA** | Protein kinase A |
| **RIPA** | Radioimmunoprecipitation assay buffer |
| **RNA** | Ribonucleic acid |
| **Rot** | Rotenone |

| | |
|---|---|
| **SDS** | Sodium dodecyl sulfate |
| **SEM** | Standard error of the mean |
| **SPF** | Specific pathogen-free |
| **siRNA** | small interfering RNA |
| **SVF** | Stromal vascular fraction |
| **TG** | Triglyceride |
| **Ucp1** | Uncoupling protein 1 |
| **WT** | Wild type |

# TABLE OF CONTENTS

# LIST OF FIGURES

# LIST OF TABLES

# INTRODUCTION

In mammals, WAT (White adipose tissue) has a unilocular droplet, lower mitochondria mass, and stores energy, on the other side, BAT has a multilocular droplet, much mitochondria mass, and increases energy expenditure (Harms and Seale, 2013; Vitali et al., 2012) (Figure 1). Brown adipocytes dissipate energy with heat generation in response to stimuli like CL-316,243 injection, cold exposure and aerobic exercise. Uncoupling protein 1 (Ucp1) is a mitochondrial protein that is well known as thermogenin, which functions to generate heat in BAT (Kajimura et al., 2015).

Inguinal white fat can be converted to beige fat by stimuli such as cold exposure, treatment with β3-adrenergic receptor (β3-AR) agonists, CL (CL-316,243), and exercise (Kaisanlahti and Glumoff, 2019). This phenomenon is referred to as the “browning” or “beiging” of white adipocytes (Ishibashi and Seale, 2010). Beige adipocytes are similar to brown adipocytes that have multilocular lipid droplets, and many mitochondria and function to dissipate energy for heat generation.

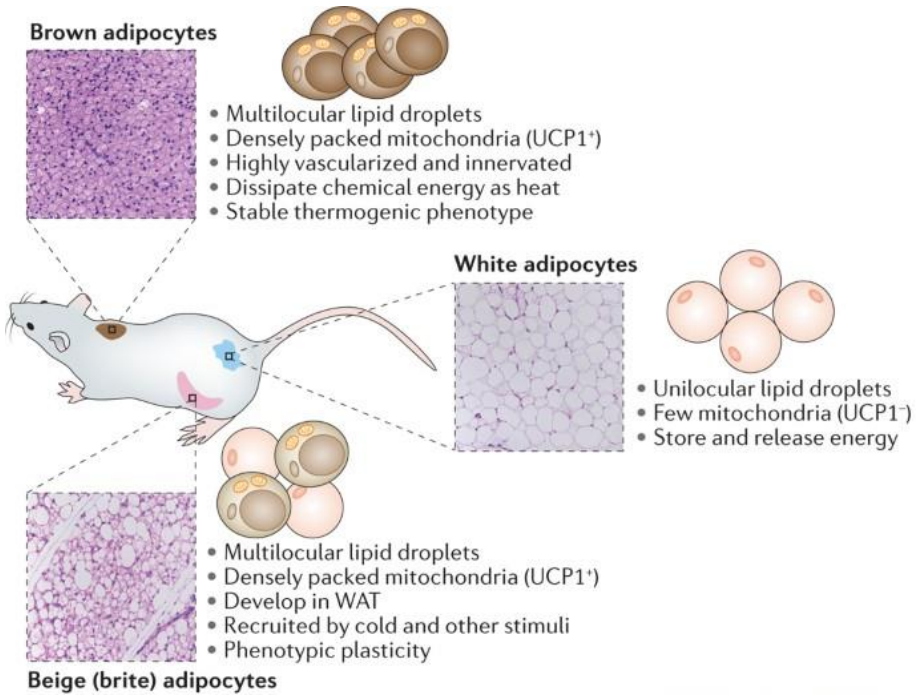


**Figure 1. White adipocytes, brown adipocytes, and beige adipocytes.**

(Wenshan Wang et al. Nat Rev Mol Cell Biolo, 2016).

CL stimulates β3-AR through coupling with the Gsα subunit and activates cyclic AMP (cAMP) production, leading to activating the protein kinase A (PKA) pathway in adipocytes (Kajimura and Saito, 2014). This process subsequently induces lipolysis that converts triacylglycerol (TG) to fatty acid (FA) via hormone-sensitive lipase (HSL) phosphorylation in adipocytes. The free fatty acid (FFA) induces ucp1 in mitochondria, which is called thermogenesis pathway (Cohen and Spiegelman, 2015) (Figure 2).

Recent several studies identified the functions of ucp1-dependent new genes in beige fat, on the other hand, few researchers revealed ucp1 independent thermogenesis (Hattori et al., 2016; Shuai et al., 2019; Zhang et al., 2020). These recent research trends have prompted me to find new genes involving to browning process.

To investigate up-regulated genes in beige adipocytes compared to white adipocytes, I performed RNA-seq analysis of iWAT upon CL challenge. I selected 97 mitochondrial genes among 292 up-regulated genes in CL challenge group. Next, I found that one of them, which is Lace1, is enriched in BAT compared to other tissues through BioGPS database.

Lace1 (Lactation elevated 1) is human homologue of yeast mitochondrial Afg1 (ATPase family gene1) ATPase, a member of the SEC18-NSF, PAS1, CDC48-VCP, TBP family (Cesnekova et al., 2016). ATPases are divided into F-ATPase, P-ATPase, and V-ATPase, of which Lace1 is classified as F0/F1 ATPase (Okuno et al., 2011). F0/F1 ATP synthase is an enzyme localized in the

inner membrane of mitochondria, where it catalyzes the synthesis of ATP from ADP (Zheng and Ramirez, 2000). Recent studies reported that ATPase regulates thermogenesis ucp1 dependent or UCP1 independent manners (Ikeda et al., 2017; Li et al., 2020b).

Lace1 is also a mitochondrial integral membrane protein that controls mitochondrial protein homeostasis (Cesnekova *et al.*, 2016). Jana Cesnekova et al. reported that Lace1 mediates degradation of nuclear-encoded complex IV subunits COX4 (cytochrome c oxidase 4), COX5A, and COX6A, and is required for normal activity of complexes III and IV of the respiratory chain.

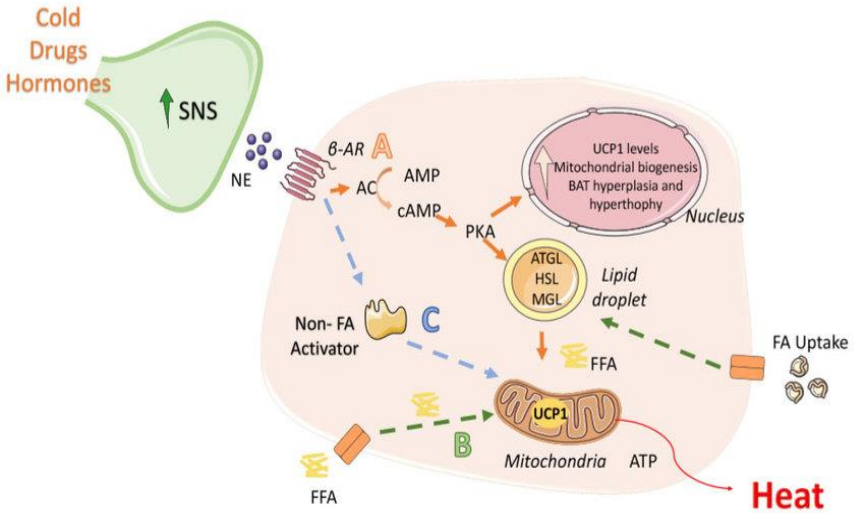


**Figure 2. Thermogenesis through the *β*-adrenergic receptor-dependent pathway in adipocytes** (Patricia Seoane-Collazo et al. Nutrients, 2020).

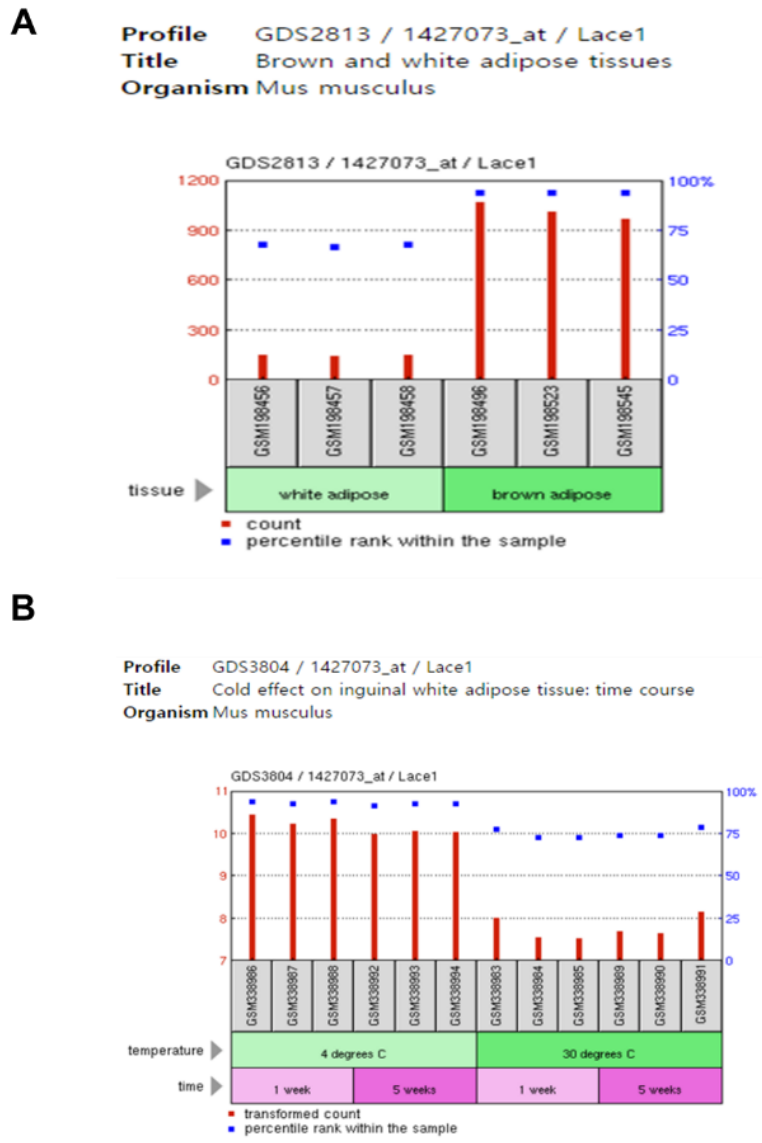


**Figure 3. GEO profile of Lace1 expression in mouse (*Mus musculus*).**

Lace1 is enriched in brown adipose tissue compared to white adipose tissue. Also, Lace1 is upregulated in iWAT of mice upon cold exposure. These data were from GDS2813 and GDS53804 from GEO (Gene expression omnibus) (Figure 3).

In this study, I confirmed that Lace1 is higher expressed in BAT tissue compared to others. Also, I identified that Lace1 is increased in white adipocytes under administering CL or exposing cold temperature or after aerobic exercise. I confirmed that Lace1 is increased during beige adipogenesis. Here, I explore browning process of iWAT in Lace1 KO mice upon CL challenge and cold exposure.

# MATERIALS AND METHODS

**Animals and Experimental design**

All animal experiments proceed according to the "Guide for Animal experiments". These animal experiments were approved by the Institutional Animal Care and Use Committee of Seoul National University, Seoul, Korea (permission number: SNU-210217-9). Lace1 KO mice were generated by gene editing with CRISPR/Cas9 by Macrogen (Korea). All animals were housed at 12 hr light/dark cycle, 22 ± 1 ℃, 50-60 % humidity, and 12 h light/dark cycle in an SPF (Specific Pathogen Free) facility. All mice were randomly assigned. To induce browning of iWAT and BAT activation, mice were treated with daily intraperitoneal injections of 1mg/kg CL-316,243 (C5976, Sigma, St. Louis, USA) for 3 days. For cold challenge, mice were housed at 6 ± 2℃ for 7 days, while control mice (warm challenge) were kept at 30 ± 2°C for 7 days. For aerobic exercise training, mice were performed voluntary wheel running exercise for 4 weeks. The daily running distance was recorded using an activity wheel running counter machine (STARR Life Science, PA, USA). For rectal temperature records after the onset of acute exhausted exercise, mice were exercised on a treadmill machine. The exhaustion exercise test protocol is presented in Table 2. The rectal temperature of mice was recorded by using a BAT-12 microprobe thermometer (Physitemp, Clifton, USA).

**Indirect Calorimetry**

$VO_2$ and energy expenditure were estimated by indirect calorimetry during CL challenge for 3 days and cold exposure (4°C) for 7 days. During measurement indirect calorimetry, all mice were housed in a single cage with free access to food and water under 12 hr light/dark cycle. All mice were monitored by PhenoMaster 7.5.6 (TSE system, Berlin, Germany) during measurement of $VO_2$ and energy expenditure.

**Analysis of Bulk-RNA sequencing and bioinformatics work**

llumina's TruSeq Stranded mRNA LT Sample Prep Kit was used to prepare RNA-Sequencing libraries and high-throughput sequencing was performed with llumina's NovaSeq 6000 Platform for each sample. Sequenced reads were mapped to GRCm39 mouse reference genome using STAR v2.7.4a. Differential expression analysis was performed using R package DESeq2 v.1.32.0 and apeglm v1.14.0 as a shrinkage method. Differentially expressed genes were identified with cutoff of adjusted-P value < 0.01 and log2 fold change > 1 in CL challenged experimental group and adjusted-P value < 0.05 and log2 fold change > 0.58 in Lace1 KO experimental group. All Graphical visualization was implemented in R using ggplot2 v3.3.5

**RNA extraction and Quantitative PCR**

For mRNA expression analysis, total RNA was extracted using TRIzol reagent (A33251, Invitrogen, MA, USA), and 1ug of RNA was used to synthesize cDNA using RT premix (K-2044-B, Bioneer, Korea). qPCR was performed using the SYBR Green Kit (BIO-92005, Meridian bioscience, OH, USA) according to the manufacturer's instructions.

All expression values were normalized to the control gene (*36B4*). The fold change for all samples was calculated by the $2^{-\Delta\Delta Ct}$ method. The primer sequences are listed in Table 1.

**Protein extraction and Western Blotting**

For protein expression analysis, all proteins were extracted using RIPA buffer (BR002, Biosolution, Korea) with protease inhibitor cocktail and phosphatase inhibitor cocktail (P3100-001, P3200-001, TX, USA). The protein concentration was determined by BCA assay kit (23227, Thermo Scientific, MA, USA). Equal amounts of proteins were separated on SDS-PAGE gels and transferred to the PVDF membrane. Antibodies for western blotting are listed in Table 1. After transfer to the PVDF membrane, the membrane was blocked by 5% skim milk based 1X TBST for 1 hr. Primary antibodies targeting the following proteins were used: LACE1 (NBP1-89215, Novus Biologicals, CO, USA), UCP1 (ab10983, Abcam), MCT1 (ab250131, abcam), MCT4 (ab74109, abcam), LDHA (2012, CST), phospho-PDH (31866, CST), PDH (3205, CST), HIF1α (36169 , CST), α-actin (A2066, Sigma-Aldrich), β-tubulin (ab2146,

abcam). The membranes were then incubated with anti-rabbit IgG horse-radish peroxidase-linked secondary antibody (PI-1000-1, Vector laboratories, CA, USA). The bands were visualized with enhanced chemiluminescence reagents (170-5061, Bio-rad, CA, USA) and the signal was analyzed with Chemi-Doc XRS+ System (Bio-rad). The levels of target protein were then normalized against the α-actin protein levels. Band intensities were measured with Image J software (NIH, MD, USA).

**Histopathology**

iWAT and BAT tissues were fixed with 4% paraformaldehyde (HP2031, Biosesang, Korea) at room temperature overnight, embedded in paraffin, and sectioned to 3-5μm. For H&E staining, all slides are stained following the manufacturer's instructions.

For immunohistochemistry (IHC) staining, slides were stained with antibody against anti-UCP1 (ab10983, abcam, UK) at 4°C overnight. All slides were stained using an HRP/DAB detection IHC kit (ab64261, Abcam). All slides were analyzed under Pannoramic Scanner (3D HISTECH, Hungary). All experiments were performed according to the manufacturer's instructions.

**Brown adipocytes cell culture**

When the brown pre-adipocyte cells reached 90-100% confluency, the cells were induced using induction medium (DMEM with 10 % FBS, 0.5 mM isobutyl methylxanthine (I7018, Sigma), 0.5 μM dexamethasone (D1756, Sigma), 125μM indomethacin (I7378, Sigma), 1nM T3 (T2877, Sigma) and 20nM insulin (sc-360248, Santa Cruz, TX, USA)). After induction for 2 days, the medium was changed to insulin medium (DMEM with 10% FBS, 1nM T3, and 20 nM insulin). The insulin medium changed every 2 days for 4 days.

**Beige adipocytes Cell culture**

Seven-weeks old male C57BL/6N mice were sacrificed to harvest SVF (Stromal vascular fraction) from iWAT. iWAT tissues were digested with 1.5u/ml Collagenase D (11088882001, Roche) at a 37 ℃ shaker for 30 mins. The SVF pellets were incubated in collagen-coated plates with maintain medium (DMEM/F12 with 10% FBS and 1X P/S) for 1 hr. After then, the medium was changed to a fresh medium for removing immune cells, etc. Once the cells reached 90-100 % confluency, the beige adipocyte differentiation was induced from pre-adipocytes of iWAT by the DMEM/F12 containing 10 % FBS, 0.5 mM isobutylmethylxanthine (I7018, Sigma), 2 μg/mL dexamethasone (D1756, Sigma), 125 μM indomethacin (I7378, Sigma), 0.5 μM rosiglitazone (R2408, Sigma), 1 nM T3 (T2877, Sigma) and 5 μg/mL insulin (sc-360248, Santa Cruz). Two days after induction, the medium was changed to the

DMEM/F12 supplemented with 10 % FBS, 0.5 μM rosiglitazone, 1 nM T3, and 5 μg/mL insulin. Four days after induction, the medium was changed to DMEM/F12 supplemented with 10% FBS, 1 μM rosiglitazone, 1 nM T3, 5 μg/mL insulin. Six days after induction, samples were harvested using TRIzol and RIPA buffer.

**RNA interference**

Five days after differentiation, brown adipocytes were transfected with 50nM Lace1 small interfering RNA (siRNA) or Negative Control siRNA for 36 hr using Lipofectamine RNAiMAX reagent (13778075, Thermo Scientific, USA) for generation Lace1 knockdown adipocytes. The pre-designed siRNA directed against murine *Lace1* mRNA (accession no. NM_001359297.1) was purchased from Bioneer (Daejeon, Korea).

**Oxygen consumption ratio (OCR)**

Brown adipocytes transfected with Lace1 siRNA were measured oxygen consumption rate (OCR) using a Seahorse Fe Extracellular Flux Analyzer (Agilent Technologies, CA, USA). For the measurement of OCR, the differentiated brown adipocytes were incubated at 37 °C non-$CO_2$ incubator for 1 hr with the Seahorse XF DMEM (103575-100, Agilent) with 1 mM pyruvate (103577-100, Agilent), 2 mM glutamine (103579-100, Agilent), and 10 mM glucose (103578-100, Agilent). After incubation, the brown adipocytes were

treated with 1.5 μM oligomycin, 2.0 μM carbonyl cyanide-4 (trifluoromethoxy) phenylhydrazone (FCCP), and 0.5 μM rotenone and antimycin (Rot/AA). All reagents were used from Agilent Seahorse XF Cell Mito Stress Test Kit (103015-100, Agilent). The OCR of brown adipocytes was normalized to the protein amounts.

**Mitochondria isolation**

Mitochondria and cytosol isolation from differentiated brown adipocytes were performed by Mitochondrial isolation kit (ab110170, abcam). $1x10^7$ brown adipoctyes were used for mitochondria isolation. Isolated mitochondria protein from brown adipocytes were extracted using RIPA buffer (BR002, Biosolution, Korea) with protease inhibitor cocktail and phosphatase inhibitor cocktail (P3100-001, P3200-001, TX, USA).

**L-Lactate measurement**

Serum L-Lactate amounts were measured by an L-lactate assay kit (ab65331, abcam). 10μl serum samples were measured using a microplate reader at OD 450nm. Final concentration of L-lactate in serum samples were calculated as:

$$\text{Lactate concentration} = \frac{\text{Amount of Lactic acid in the sample well calculated from standard curve (nmol)}}{\text{Volume of sample added into the well (μl)}} \text{ x (Sample dilution factor)}$$

**ATP assay**

ATP amounts of fully differentiated brown adipocytes were analyzed using an ATP assay kit (K354-100, BioVision, CA, USA). $1x10^6$ brown adipoctyes were measured using a microplate reader at OD 570nm. Final concentration of ATP amount in brown adipocytes was calculated as:

$$\text{ATP amount} = \frac{\text{ATP amount in the reaction well from standard curve (nmol)}}{\text{Sample volume added into sample wells (µl)}} \text{ x (Sample dilution factor)}$$

**Statistical analysis**

All statistical analysis was analyzed using GraphPad Prism 7.0 (GraphPad Software, La Jolla, CA, USA). All data are presented as mean ± standard errors of the mean (SEM). Statistical significance was analyzed by an unpaired t-test. Statistical significance was determined at *$p<0.05$, ** $p<0.01$ and ***$p<0.001$.

**Table 1. Primers used for qRT-PCR analysis**

| Target gene | | Sequence (5'→3') |
|---|---|---|
| *Lace1* | Forward | CCGAGGAAATCAGTCAAGAA (20 mer) |
| *Lace1* | Reverse | GGTGGTCTGTTGGATGTT (18 mer) |
| *Ucp1* | Forward | ACTGCCACACCTCCAGTCATT (21 mer) |
| *Ucp1* | Reverse | CTTTGGCTCACTCAGGATTGG (21 mer) |
| *Cidea* | Forward | ATCACAACTGGCCTGGTTACG (21 mer) |
| *Cidea* | Reverse | TACTACCCGGTGTCCATTTCT (21 mer) |
| *Elovl3* | Forward | TTCTCACGCGGGTTAAAAATGG (22 mer) |
| *Elovl3* | Reverse | GAGCAACAGATAGACGACCAC (21 mer) |
| *Cox8b* | Forward | GAACCATGAAGCCAACGACT (20 mer) |
| *Cox8b* | Reverse | GCGAAGTTCACAGTGGTTCC (20 mer) |
| *Cox7a1* | Forward | CAGCGTCATGGTCAGTCTGT (20 mer) |
| *Cox7a1* | Reverse | AGAAAACCGTGTGGCAGAGA (20 mer) |
| *Dio2* | Forward | CAGTGTGGTGCACGTCTCCAATC (23 mer) |
| *Dio2* | Reverse | TGAACCAAAGTTGACCACCAG (21 mer) |
| *Idha* | Forward | TATCTTAATGAAGGACTTGGCGGATGAG (28 mer) |
| *Idha* | Reverse | GGAGTTCGCAGTTACACAGTAGTC (24 mer) |
| *Idhb* | Forward | TTGTGGCCGATAAAGATTACTCTGTGAC (28 mer) |
| *Idhb* | Reverse | AGGAATGATGAACTTGAACACGTTGAC (27 mer) |
| *Mct1* | Forward | CATTGGTGTTATTGGAGGTC (20 mer) |
| *Mct1* | Reverse | GAAAGCCTGATTAAGTGGAG (20 mer) |
| *Mct4* | Forward | TCAATCATGGTGCTGGGACT (20 mer) |
| *Mct4* | Reverse | TGTCAGGTCAGTGAAGCCAT (20 mer) |
| *Hcar1* | Forward | GCTTACCCCTTCGGACAGAC (20 mer) |
| *Hcar1* | Reverse | ATGCTCCCGGCCCTATTCA (19 mer) |

**Table 2. Acute exhausted exercise protocol**

| Step | Start Speed m/sec | End Speed m/sec | Period sec |
|---|---|---|---|
| 1 | 0.00 | 0.17 | 600 |
| 2 | 0.17 | 0.20 | 120 |
| 3 | 0.20 | 0.20 | 120 |
| 4 | 0.20 | 0.23 | 120 |
| 5 | 0.23 | 0.23 | 120 |
| 6 | 0.23 | 0.27 | 120 |
| 7 | 0.27 | 0.27 | 120 |
| 8 | 0.27 | 0.30 | 120 |
| 9 | 0.30 | 0.30 | 120 |
| 10 | 0.30 | 0.33 | 120 |
| 11 | 0.33 | 0.33 | 120 |
| 12 | 0.33 | 0.37 | 120 |
| 13 | 0.37 | 0.37 | 120 |
| 14 | 0.37 | 0.40 | 120 |
| 15 | 0.40 | 0.40 | 120 |
| 16 | 0.40 | 0.43 | 120 |
| 17 | 0.43 | 0.43 | 120 |
| 18 | 0.43 | 0.47 | 120 |
| 19 | 0.47 | 0.47 | 120 |
| 20 | 0.47 | 0.50 | 120 |
| 21 | 0.50 | 0.50 | 120 |
| 22 | 0.50 | 0.53 | 120 |
| 23 | 0.53 | 0.53 | 120 |
| 24 | 0.53 | 0.57 | 120 |
| 25 | 0.57 | 0.57 | 120 |
| 26 | 0.57 | 0.60 | 120 |
| 27 | 0.60 | 0.60 | 120 |
| 28 | 0.60 | 0.63 | 120 |
| 29 | 0.63 | 0.63 | 120 |
| 30 | 0.63 | 0.67 | 120 |
| 31 | 0.67 | 0.67 | 120 |
| 32 | 0.67 | 0.70 | 120 |
| 33 | 0.70 | 0.70 | 120 |
| 34 | 0.70 | 0.73 | 120 |
| 35 | 0.73 | 0.73 | 120 |
| 36 | 0.73 | 0.77 | 120 |

# RESULTS

### 1. Lace1 is a mitochondrial ATPase highly expressed in BAT

I compared CL-treated and non-treated mice using the bulk RNA-seq technique to investigate novel genes in beige adipogenesis. Among 292 upregulated differentially expressed genes (DEGs) during CL challenge (adjusted-P value < 0.01 and fold change > 2 as cutoff), 97 were recognized as non-browning mitochondrial genes annotated as mitochondrial genes (GO:0005739) but unannotated for the browning related biological process (GO:1990845, GO:0070342, GO:0050873, KEGG PATHWAY: mmu04714). Eleven genes highly expressed in BAT were identified using the BioGPS database as the criteria for narrowing down candidate genes of interest. This study presented Lace1, a highly enriched non-browning mitochondrial gene in BAT, as a novel gene in beige adipogenesis (Figure. 4 A-B).

I first determined the expression levels of Lace1 in whole tissue of 7-week-old C57BL/6N male mice. *Lace1* mRNA was more expressed in BAT than in other tissues (Figure. 5 A). Additionally, the expression of LACE1 protein was highest in BAT, followed by heart, soleus, and kidney tissue (Figure. 5 B).

After then, I identified Lace1 expression during brown adipogenesis using immortalized brown pre-adipocyte. As a result, the LACE1 protein level increased during brown adipogenesis as with UCP1 and peroxisome proliferator-activated receptor gamma coactivator 1-alpha (PGC1α) (Figure. 6

A). *Lace1* mRNA also increased during brown adipogenesis with *Ucp1*, Cell death-inducing DNA fragmentation factor alpha-like effector A (*Cidea*), and *Pgc1α* mRNA in an expression-dependent manner (Figure. 6 B-E). Next, I induced beige adipogenesis using pre-adipocytes isolated from iWAT in 7-week-old male C57BL/6N mice. During beige adipogenesis, the LACE1 protein level increased as with UCP1 (Figure. 7 A). Additionally, *Lace1* mRNA increased during beige adipogenesis in a *Ucp1* mRNA-expression-dependent manner (Figure. 7 B).

Next, I confirmed the expression of Lace1 in the cytosol and mitochondria of pre-adipocyte and fully differentiated brown adipocytes using immortalized brown pre-adipocytes to identify the localization of Lace1 expression (Aune *et al.*, 2013). LACE1 protein was expressed only in the mitochondria of fully differentiated brown adipocytes (Figure. 8 A). Therefore, I transfected with siRNA directed against the Lace1 gene in fully differentiated brown adipocytes. After transfection with siLace1, I confirmed the mitochondrial function in fully differentiated brown adipocytes by directly measuring the OCR. I found that the OCR of the Lace1 knockdown (KD) group in brown adipocytes was lower than that of the control siRNA group (Figure. 9 A). In particular, the basal and maximal respiration rate of brown adipocytes tend to be lower in Lace1 KD than in WT (Figure. 9 B-E). Lace1, also known as mitochondrial ATPase, synthesizes ATP (Cesnekova *et al.*, 2016). I confirmed that the ATP level is lower in Lace1 KD brown adipocytes than in WT (Figure. 10 A).

These findings suggest that Lace1 is highly expressed in mouse BAT and increased during brown adipogenesis and beige adipogenesis.

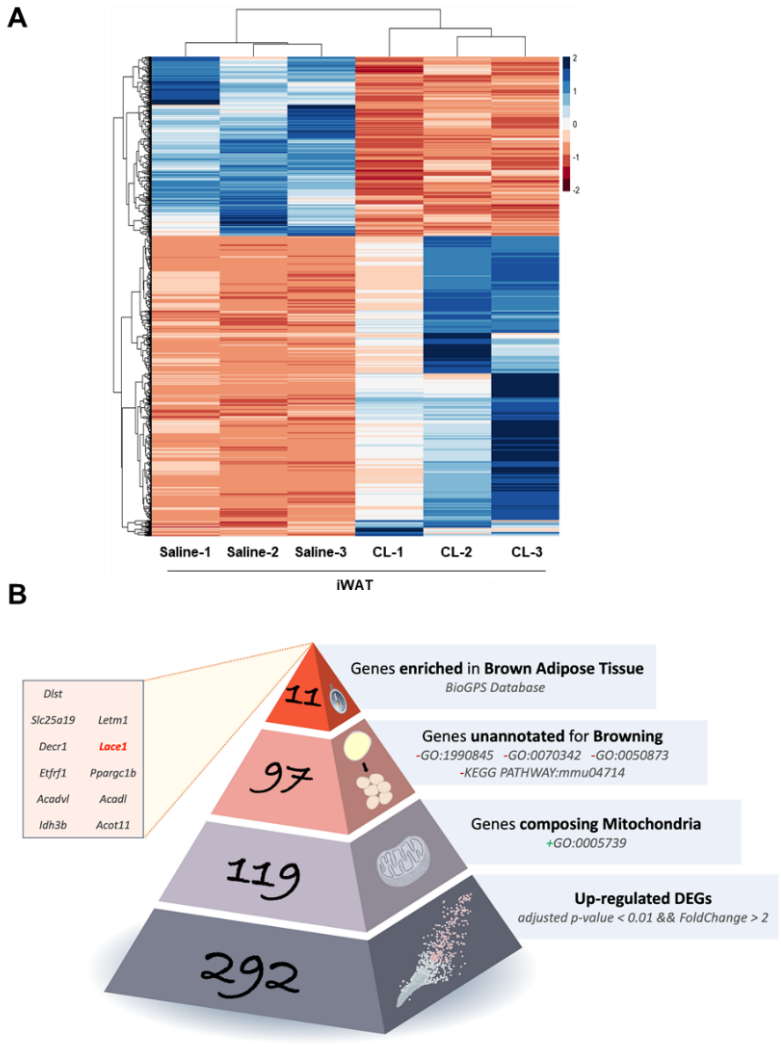


**Figure 4. Transcriptomic analysis of up-regulated genes in iWAT under CL challenge.**

(A) Hierarchical clustering and heat map of bulk-RNA sequencing in iWAT upon CL challenge. The color scale represents the Z-score of regularized log transformation of read counts. It means the relative mRNA expression value of each gene in blue (low expression)-white-red (high expression); n=3 for all group. (B) Among 292 upregulated differentially expressed genes (DEGs) upon CL challenge (P value < 0.01, fold change > 2 as cutoff), 119 were annotated as mitochondrial genes (GO:0005739), 97 were recognized as non-browning mitochondrial genes, and 11 were enriched in brown adipose tissue. One of these 11 genes is Lace1.

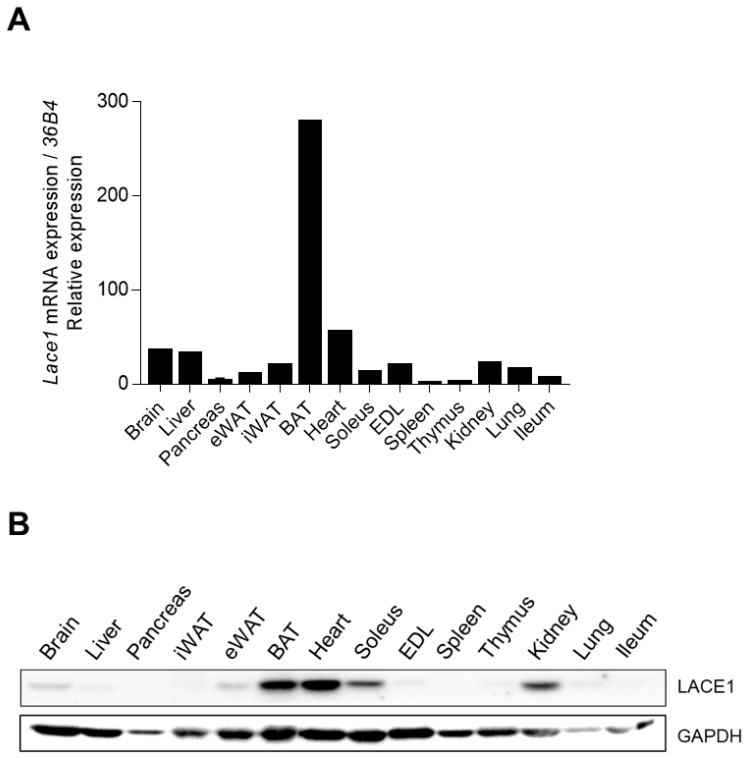


**Figure 5. Lace1 expression in whole tissue of mice.**

(A) *Lace1* mRNA expression in whole tissue of mice; n=4 per group. (B) LACE1 protein expression in whole tissue of mice; n=4 per group. All experiments were performed after intervention. Values are shown as means ± SEM.

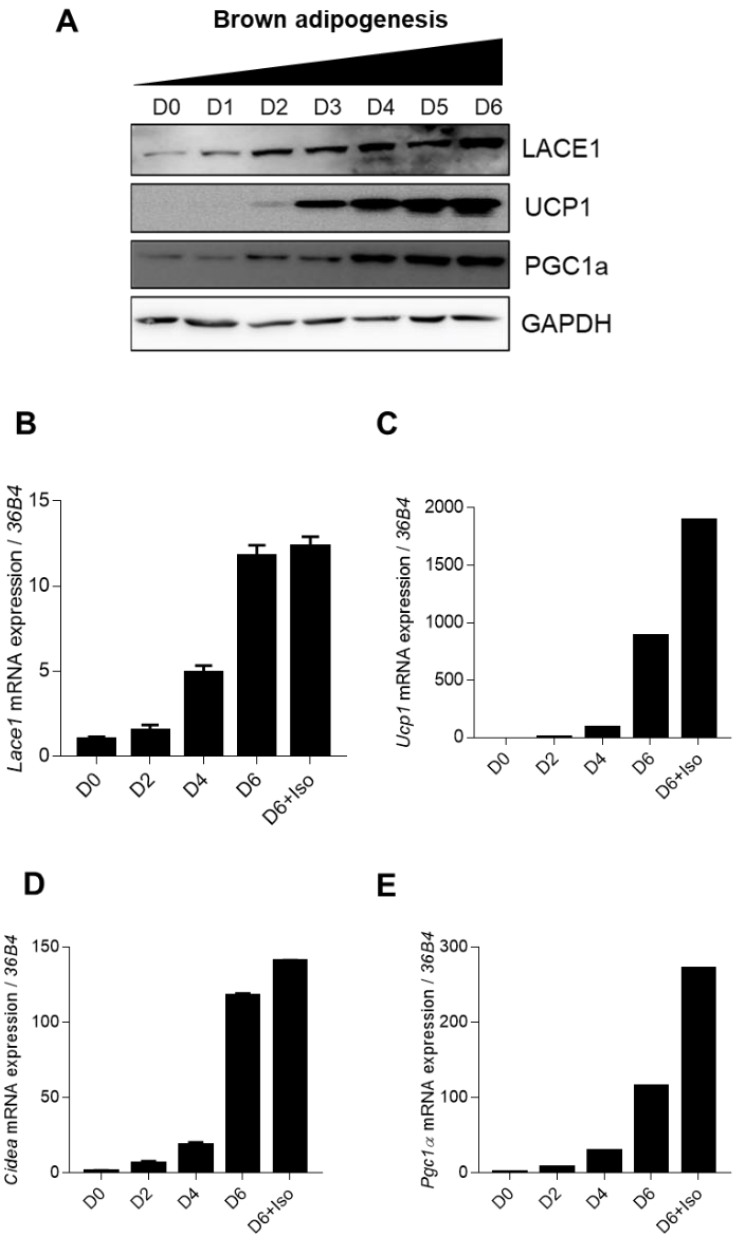


**Figure 6. Lace1 expression during brown adipogenesis.**

(A) LACE1, UCP1, and PGC1α protein expression during brown adipogenesis. (B) *Lace1* mRNA expression during brown adipogenesis; n=3 for all group. (C) *Ucp1* mRNA expression during brown adipogenesis; n=3 for all group. (D) *Cidea* mRNA expression during brown adipogenesis; n=3 for all group. (E) *Pgc1α* mRNA expression during brown adipogenesis; n=3 for all group. All experiments were performed after intervention. Values are shown as mean ± SEM.

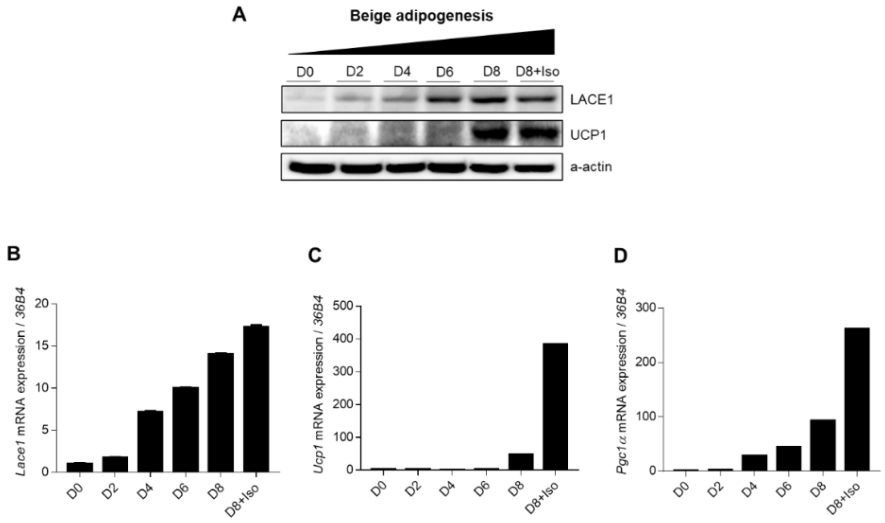


**Figure 7. Lace1 expression during beige adipogenesis.**

(A) LACE1 protein expression during beige adipogenesis. (B) *Lace1* mRNA expression during beige adipogenesis; n=3 for all group (C) *Ucp1* mRNA expression during beige adipogenesis; n=3 for all group. (D) *Pgc1α* mRNA expression during beige adipogenesis; n=3 for all group. All experiments were performed after intervention. Values are shown as mean ± SEM.

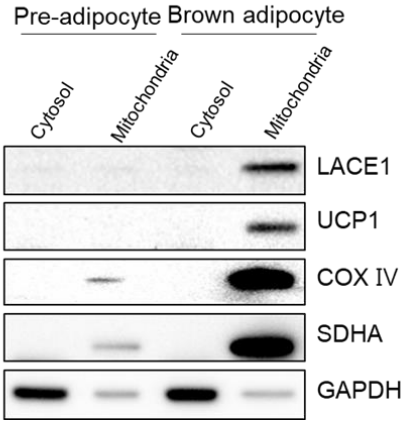


**Figure 8. Lace1 expression in the cytosol and mitochondrial of pre-adipocytes and brown adipocytes.**

LACE1, UCP1, COX IV, SDHA, and GAPDH protein expression in cytosol and mitochondria of pre-brown adipocytes and fully differentiated brown adipocytes using immortalized brown pre-adipocytes (iBPA) cell lines.

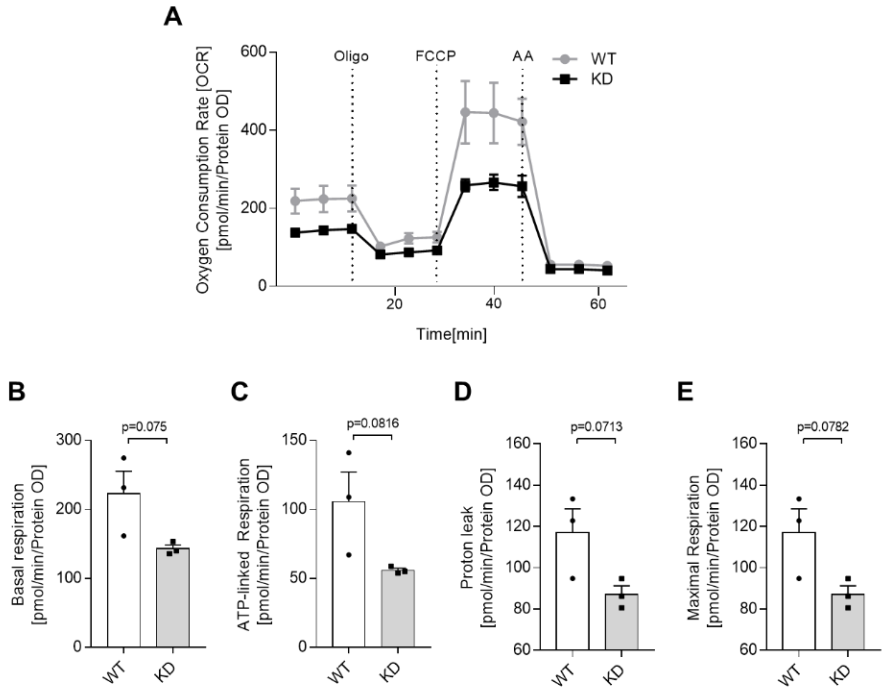


**Figure 9. Oxygen consumption rate (OCR) of Lace1 KD (Knock down) in fully differentiated brown adipocytes.**

(A) OCRs of Lace1 knock down (KD) in fully differentiated brown adipocytes of iBPA cell line. (B) Basal respiration of Lace1 KD in fully differentiated brown adipocyte of iBPA cell line. (C) ATP-linked respiration of Lace1 KD in fully differentiated brown adipocyte of iBPA cell line. (D) Proton leak of Lace1 KD in fully differentiated brown adipocyte of iBPA cell line. (E) Maximal respiration of Lace1 KD in fully differentiated brown adipocyte of iBPA cell line. (A-E) n=3 for all group. All experiments were performed after intervention. Values are shown as mean ± SEM. Significance was calculated using unpaired two-tailed student's t-test.

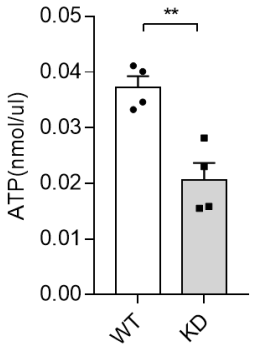


**Figure 10. Lace1 functions to ATP synthesis**.

ATP level of Lace1 KD in fully-differentiated brown adipocytes of iBPA cell line; n=4 for all group. All experiments were performed after intervention. Values are shown as mean ± SEM. Significance was calculated using unpaired two-tailed student's t-test. *p<0.05, **p<0.01, ***p< 0.001

**2. Lace1 increased in iWAT and BAT following CL challenge, cold exposure, and exercise**

My transcriptomic data revealed that the Lace1 gene is upregulated in iWAT under CL challenge (Figure. 4). Therefore, I hypothesized that Lace1 increased in beige fat following Ucp1 in an expression-dependent manner and was upregulated during beige adipogenesis. I confirmed that *Lace1* mRNA levels increased as with thermogenic genes (Figure. 11 B-C). LACE1 protein is also increased in CL-induced beige fat as with UCP1 (Figure. 11 D-E). Additionally, Lace1 mRNA and protein tended to be increased in BAT, but not significantly (Figure. 12 B-E).

Subsequently, I investigated Lace1 expression under cold exposure. Cold exposure induced iWAT browning via the release of norepinephrine and β3-adrenergic stimulation (Bargut et al., 2017; Chartoumpekis et al., 2011). Consequently, *Lace1* mRNA increased as with thermogenic genes (Figure. 13 B-C). Likewise, LACE1 protein increased in cold-induced beige fat compared with white fat (Figure. 13 D-E). Lace1 mRNA and protein expression levels are also increased in BAT upon cold exposure (Figure. 14 B-E). I found that Lace1 increased in a Ucp1-dependent manner under CL challenge and cold exposure. These data suggested that Lace1 increased in iWAT under browning stimuli in a Ucp1-expression-dependent manner.

Next, I confirmed that *Lace1* mRNA is increased in iWAT after voluntary aerobic wheel running exercise for 4-weeks (Figure. 15 B-C). The LACE1 protein level is also increased in iWAT following UCP1 in an expression-dependent manner (Figure. 15 D-E). Lace1 mRNA and protein tended to be increased in BAT (Figure. 16 B-E).

These findings suggest that Lace1 was upregulated in iWAT under CL challenge, cold exposure, and wheel running exercise.

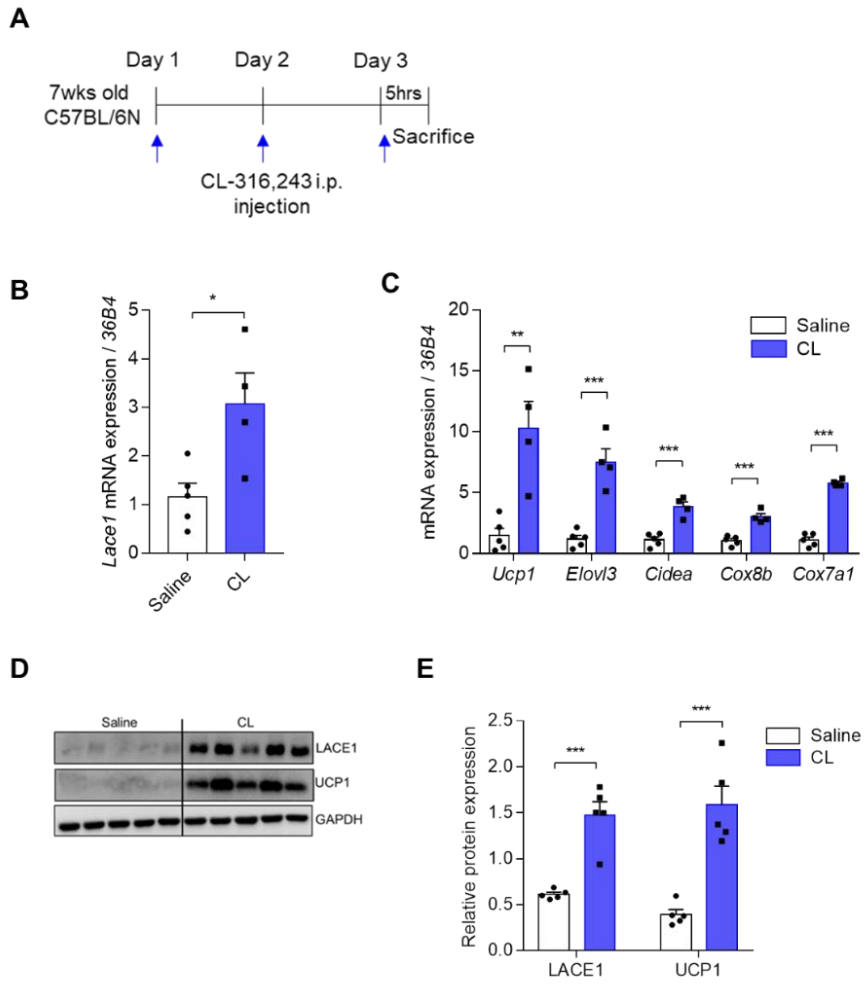


**Figure 11. Lace1 is increased in iWAT in a UCP1-dependent manner by CL injection.**

(A) Experimental design. To induce browning of iWAT and BAT activation, mice were treated with daily intraperitoneal injections of 1mg/kg CL-316,243 for 3 days. (B) *Lace1* mRNA expression in iWAT under CL challenge. Saline, n=5; CL, n=4. (C) Thermogenesis-related gene expression in iWAT under CL challenge. Saline, n=5; CL, n=4. (D-E) LACE1 and UCP1 protein expression in iWAT under CL challenge. Saline, n=5; CL, n=4. Protein expression is quantified by GAPDH expression. All experiments were performed after intervention. Values are shown as means ± SEM. Significance calculated using unpaired two-tailed student's t-test. *$p < 0.05$, **$p < 0.01$, ***$p < 0.001$.

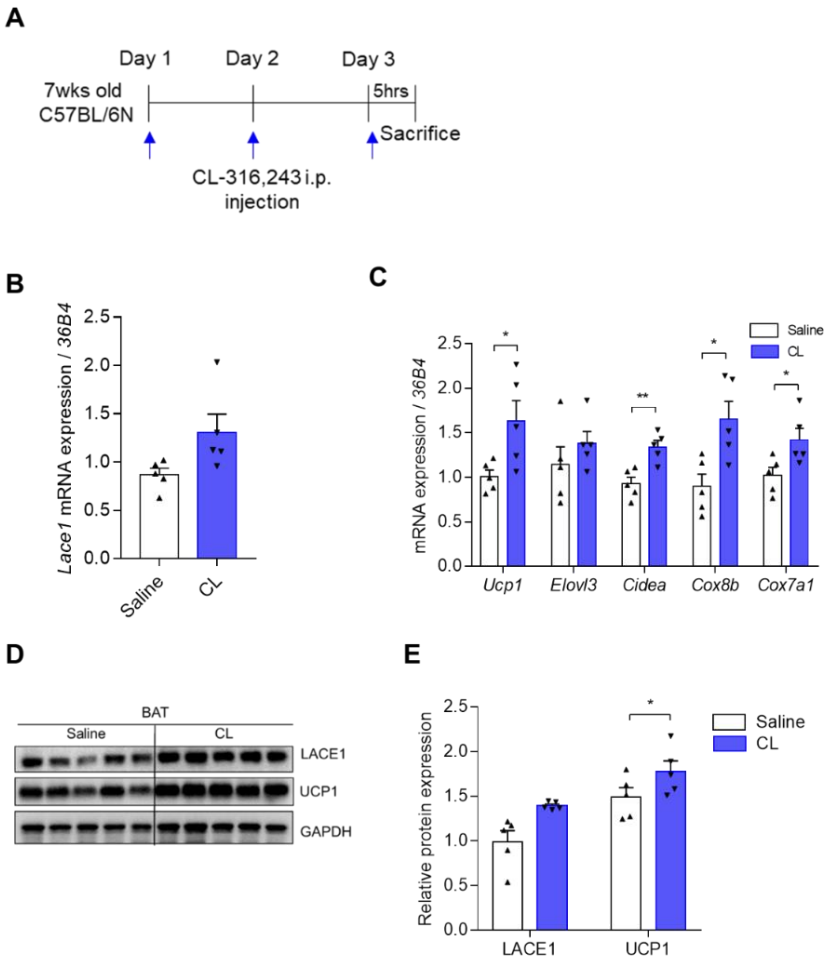


**Figure 12. Lace1 tends to be increased in BAT in by CL injection.**

(A) Experimental design. To induce browning of iWAT and BAT activation, mice were treated with daily intraperitoneal injections of 1mg/kg CL-316,243 for 3 days. (B) *Lace1* mRNA expression in BAT under CL challenge. n=5 for all group. (C) Thermogenesis-related gene expression in BAT under CL challenge. n=5 for all group. (D-E) LACE1 and UCP1 protein expression in BAT under CL challenge. n=5 for all group. Protein expression is quantified by GAPDH expression. All experiments were performed after intervention. Values are shown as means ± SEM. Significance calculated using unpaired two-tailed student's t-test. *$p < 0.05$, **$p < 0.01$, ***$p < 0.001$.

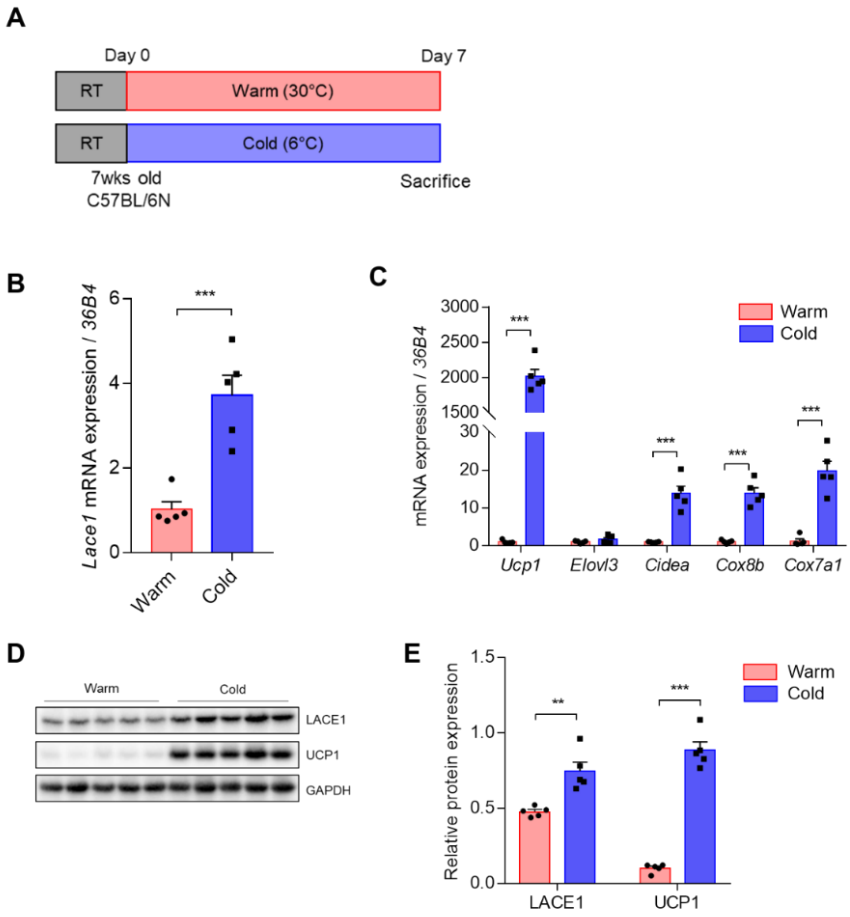


**Figure 13. Lace1 is increased in iWAT in a UCP1-dependent manner upon cold exposure.**

(A) Experimental design. For cold challenge, mice were housed at 6 ± 2°C for 7 days, while control mice (warm challenge) were kept at 30 ± 2°C for 7 days. (B) *Lace1* mRNA expression in iWAT under cold exposure; n=5 for all group. (C) Thermogenesis-related gene expression in iWAT under cold exposure; n=5 for all group. (D-E) LACE1 and UCP1 protein expression in iWAT under cold exposure; n=5 for all group. Protein expression is quantified by GAPDH expression. All experiments were performed after intervention. Values are shown as means ± SEM. Significance calculated using unpaired two-tailed student's t-test. *$p < 0.05$, **$p < 0.01$, ***$p < 0.001$.

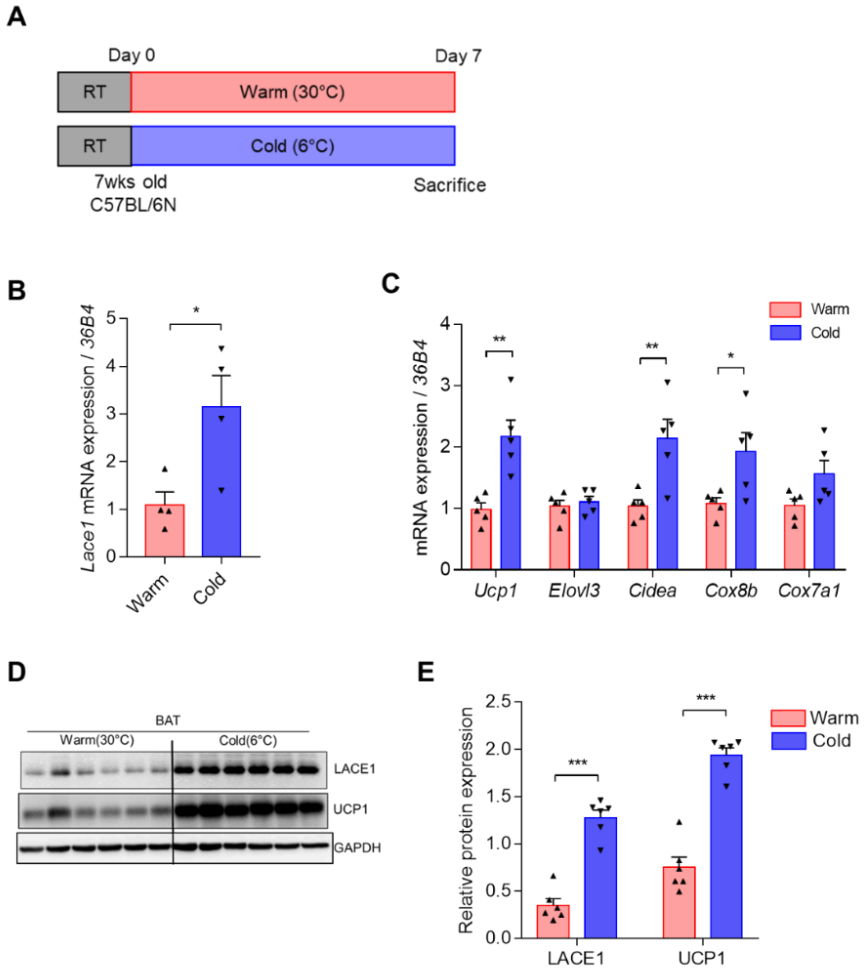


**Figure 14. Lace1 is increased in BAT in upon cold exposure.**

(A) Experimental design. For cold challenge, mice were housed at 6 ± 2°C for 7 days, while control mice (warm challenge) were kept at 30 ± 2°C for 7 days. (B) *Lace1* mRNA expression in BAT under cold exposure; n=4 for all group. (C) Thermogenesis-related gene expression in BAT under cold exposure; n=5 for all group. (D-E) LACE1 and UCP1 protein expression in BAT under cold exposure; n=6 for all group. Protein expression is quantified by GAPDH expression. All experiments were performed after intervention. Values are shown as means ± SEM. Significance calculated using unpaired two-tailed student's t-test. *$p < 0.05$, **$p < 0.01$, ***$p < 0.001$.

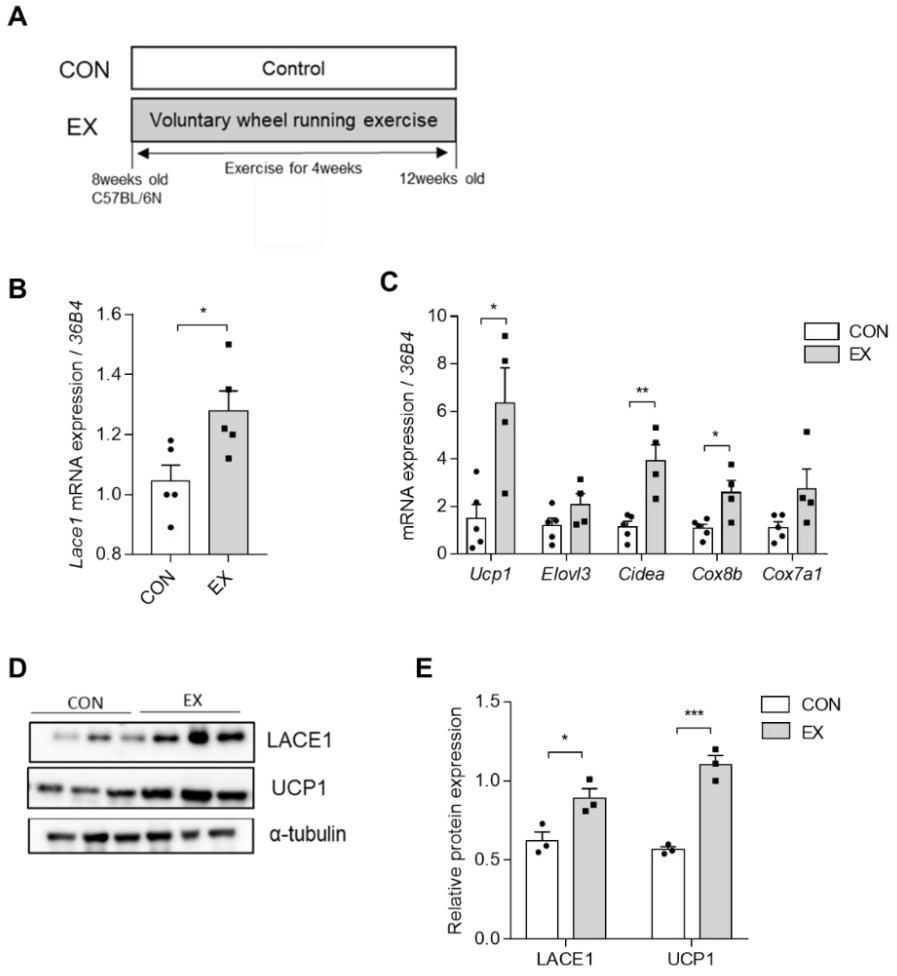


**Figure 15. Lace1 is increased in iWAT in a UCP1-dependent manner after voluntary wheel running exercise training.**

(A) Experimental design. For aerobic exercise training, mice were performed voluntary wheel running exercise for 4 weeks. The daily running distance was recorded using an activity wheel running counter machine. (B) *Lace1* mRNA expression in iWAT after wheel running exercise; n=5 for all group. (C) Thermogenesis-related gene expression in iWAT after wheel running exercise. CON, n=5; EX, n=4. (D-E) LACE1 and UCP1 protein expression in iWAT after wheel running exercise; n=3 for all group. Protein expression is quantified by GAPDH expression. All experiments were performed after intervention. Values are shown as means ± SEM. Significance calculated using unpaired two-tailed student's t-test. *$p < 0.05$, **$p < 0.01$, ***$p < 0.001$.

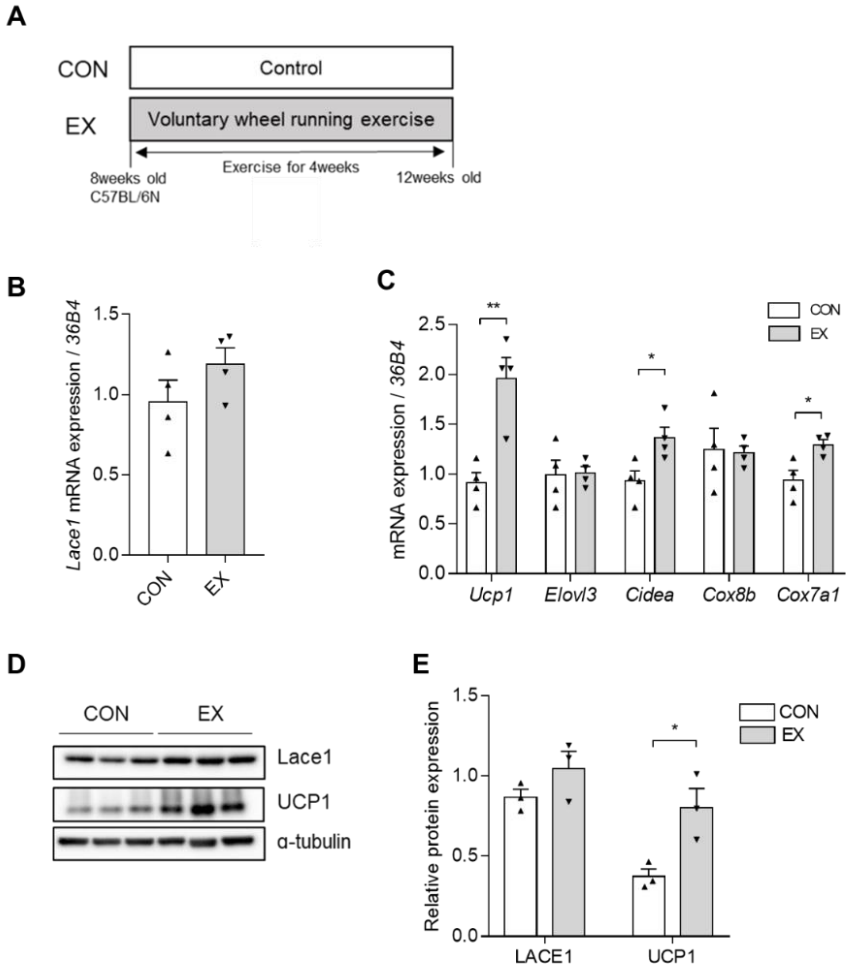


**Figure 16. Lace1 tends to be increased in BAT after wheel running exercise.**

(A) Experimental design. For aerobic exercise training, mice were performed voluntary wheel running exercise for 4 weeks. The daily running distance was recorded using an activity wheel running counter machine. (B) *Lace1* mRNA expression in BAT after wheel running exercise; n=4 for all group. (C) Thermogenesis-related gene expression in BAT after wheel running exercise; n=4 for all group. (D-E) LACE1 and UCP1 protein expression in BAT after wheel running exercise; n=3 for all group. Protein expression is quantified by α-tubulin expression. All experiments were performed after intervention. Values are shown as means ± SEM. Significance calculated using unpaired two-tailed student's t-test. *$p < 0.05$, **$p < 0.01$, ***$p < 0.001$.

### 3. Lace1 deficiency results in increased iWAT browning following CL injection

I generated Lace1 null knockout (KO) mice using the CRISPR-CAS9 system to investigate the role of Lace1 in beige fat. The Lace1 KO mouse scheme is presented in Figure. 17 A. I administered CL to Lace1 KO mice according to the experimental design (Figure. 18 A). First, I confirmed that *Lace1* mRNA expression was downregulated in Lace1 KO mouse iWAT compared to WT despite CL injection (Figure. 18 B). Subsequently, I examined the browning capacity of iWAT in Lace1 KO mice under CL challenge and found that thermogenic marker-gene level is increased in CL-induced beige fat of Lace1 KO mice compared with control littermates (Figure. 18 C). Additionally, I found that they displayed higher UCP1 protein expression than WT in iWAT under CL challenge (Figure. 18 D). Histological analysis indicated that Lace1 KO mice showed higher beige fat content than WT when challenged with CL (Figure. 18 E), and UCP1 immunostaining analysis revealed that Lace1 KO showed more UCP1-positive adipocytes than WT under CL challenge (Figure. 18 F). Also, browning activation tended to be increased in BAT of Lace1 KO mice under CL challenge, but not significantly (Figure. 19 C-F).

Ucp1 is critical for maintaining core temperature and increasing energy expenditure (Cypess and Kahn, 2010). When Ucp1 is allowed proton re-entry into mitochondria under browning stimuli such as cold exposure, oxygen

consumption is partially uncoupled from ATP synthesis because fewer protons go through F0/F1 ATP synthase (Krauss et al., 2005). CL challenge and cold exposure dependent $VO_2$ are dependent on Ucp1 activity (Inokuma et al., 2006). I used indirect calorimetric measurements to investigate the systemic metabolic phenotype with increased browning of white adipose tissue in Lace1 KO mice under CL challenge and found that oxygen consumption (Figure. 20 A-B) and heat generation (Figure. 20 C-D) increased. I hypothesized that browning capacity was decreased in iWAT by Lace1 deletion compared with WT because Lace1 was upregulated in iWAT under browning stimuli such as Ucp1; however, I found that Lace1 deficiency increased the browning capacity of iWAT under CL challenge. Based on these findings, I explored whether this phenotype was also exhibited in Lace1 KO mice under cold exposure.

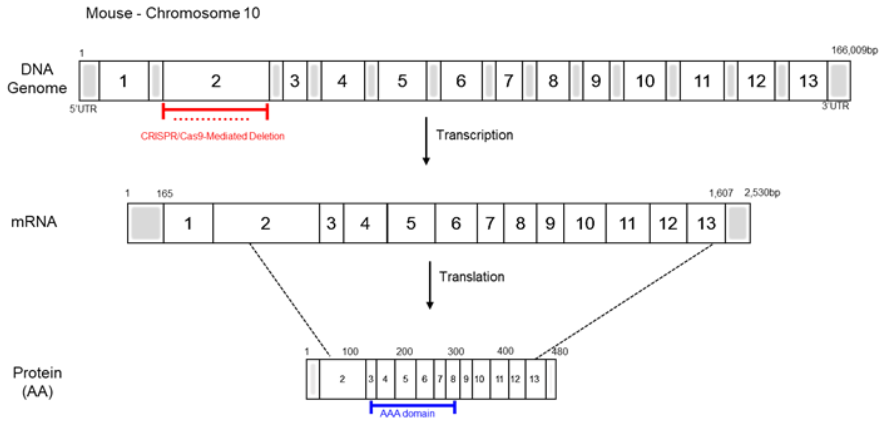


**Figure 17. Generation of Lace1 null KO mice.**

Lace1 KO mice were generated by gene editing with CRISPR/Cas9

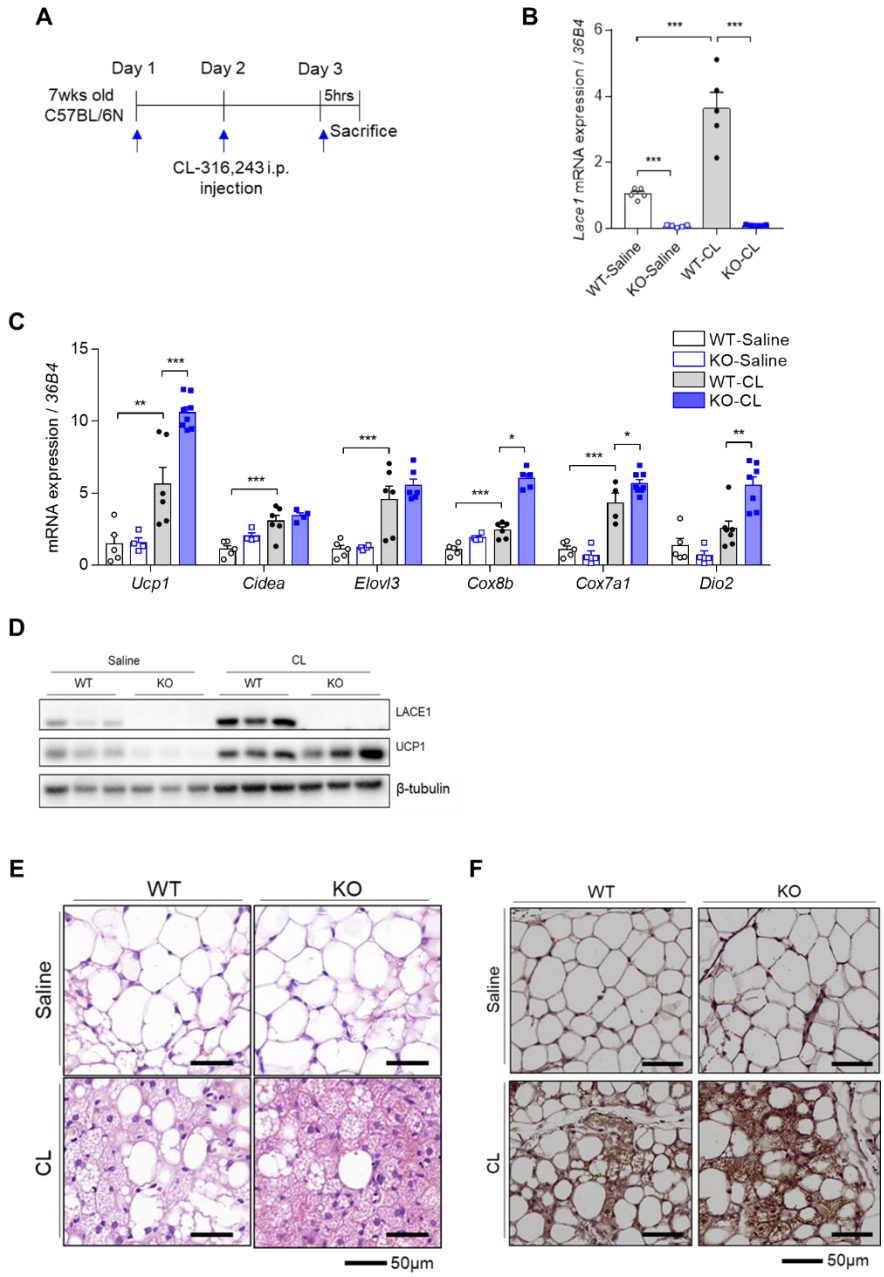


**Figure 18. Increased browning of iWAT in Lace1 KO mice upon CL injection.**

(A) Scheme of CL challenge once a day for 3 days. (B) *Lace1* mRNA expression in iWAT of Lace1 KO mice under CL challenge; n=5 for all group. (C) Thermogenesis-related gene expression in iWAT of Lace1 KO under CL challenge. WT-Saline, n = 5; KO-Saline, n = 4; WT-CL, n = 6; KO-CL, n = 6-8. (D) LACE1 and UCP1 protein expression in iWAT of Lace1 KO mice under CL challenge; n = 3 for all groups. (E) Representative H&E staining of iWAT in Lace1 KO mice under CL challenge (scale bar: 50 μm); n = 3 for all groups. (F) UCP1 immunohistochemistry staining of iWAT in Lace1 KO mice under CL challenge (scale bar: 50 μm); n = 3 for all groups. All experiments performed after intervention. Values are shown as mean ± SEM. Significance calculated using unpaired two-tailed student's t-test. *$p < 0.05$, **$p < 0.01$, ***$p < 0.001$.

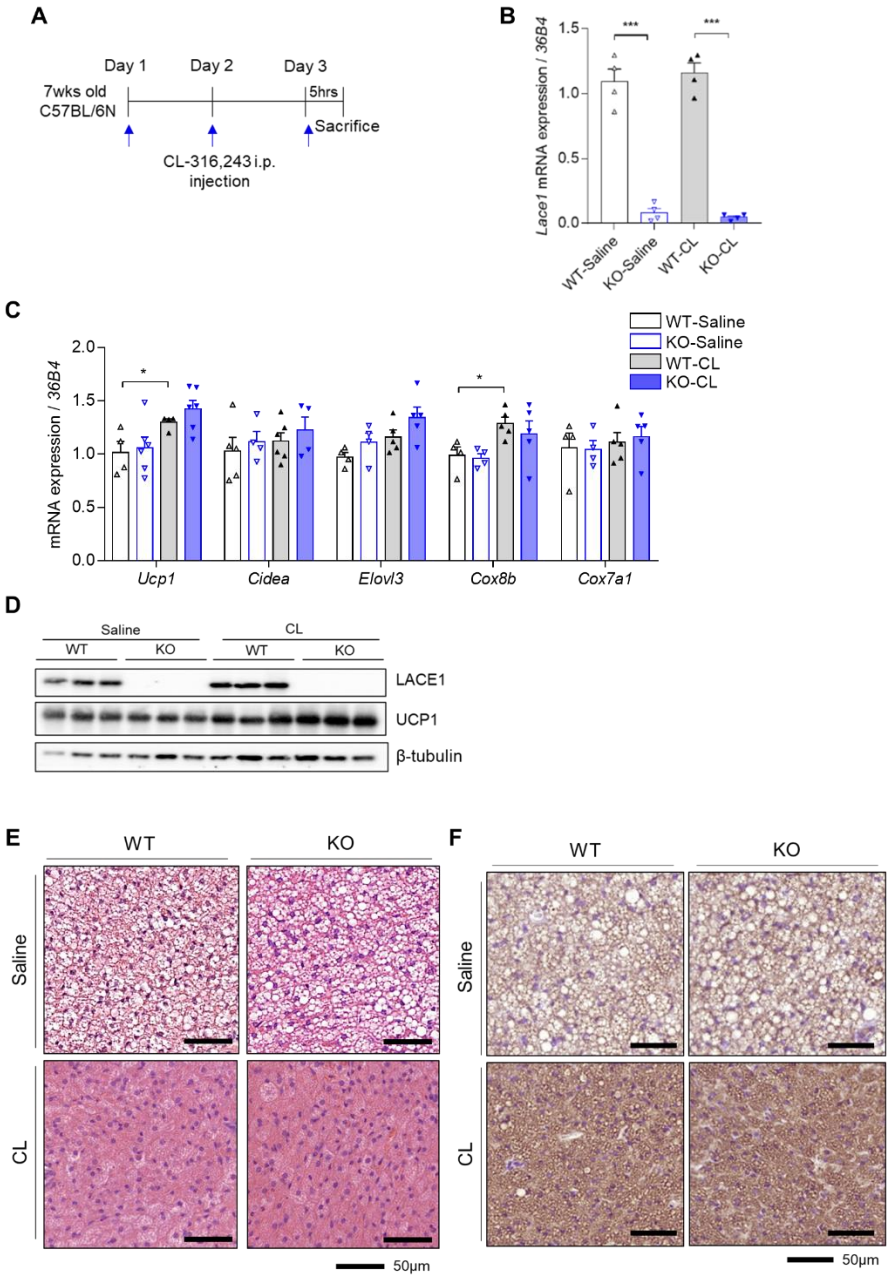


**Figure 19. BAT activation in Lace1 KO mice upon CL injection.**

(A) Scheme of CL challenge once a day for 3 days. (B) *Lace1* mRNA expression in BAT of Lace1 KO mice under CL challenge; n=4 for all group. (C) Thermogenesis-related gene expression in BAT of Lace1 KO under CL challenge. WT-Saline, n = 4-5; KO-Saline, n = 4; WT-CL, n = 6; KO-CL, n = 4-5. (D) LACE1 and UCP1 protein expression in BAT of Lace1 KO mice under CL challenge; n = 3 for all groups. (E) Representative H&E staining of BAT in Lace1 KO mice under CL challenge (scale bar: 50 μm); n = 3 for all groups. (F) UCP1 immunohistochemistry staining of BAT in Lace1 KO mice under CL challenge (scale bar: 50 μm); n = 3 for all groups. All experiments were performed after intervention. Values are shown as mean ± SEM. Significance calculated using unpaired two-tailed student's t-test. *$p < 0.05$, **$p < 0.01$, ***$p < 0.001$.

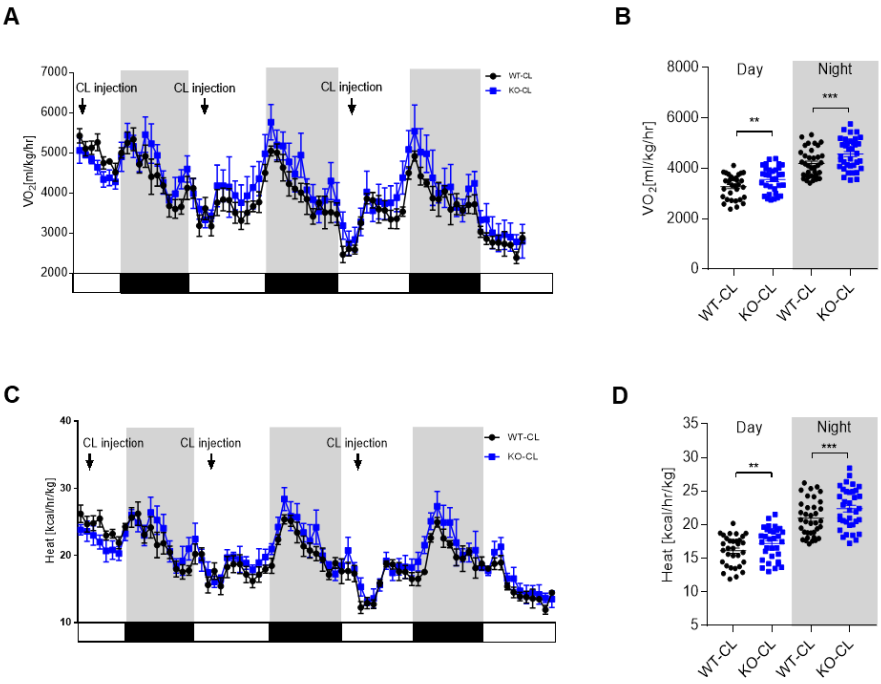


**Figure 20. Increased energy expenditure in Lace1 KO mice upon CL injection.**

Whole-body $VO_2$ and (A-B) heat generation (C-D) in Lace1 KO under CL challenge for 3 days; n = 5 for all groups. All experiments were performed after intervention. Values are shown as mean ± SEM. Significance calculated using unpaired two-tailed student's t-test. *p < 0.05, **p < 0.01, ***p < 0.001.

**4. Lace1 deficiency results in increased iWAT browning following cold exposure**

Mice were exposed to cold at 4-6 ℃ for 7 days (Figure. 21 A) to investigate the Lace1 KO mouse phenotype under cold stimuli. As shown in Figure 21 C, thermogenesis-related gene levels increased in Lace1 KO mice iWAT compared with WT mice under cold exposure. Additionally, Lace1 KO mice displayed higher UCP1 protein levels in iWAT than littermate controls under cold exposure. (Figure. 21 D). Histological analysis indicated that Lace1 KO mice had more beige fat than WT under cold exposure (Figure. 21 E), and Ucp1 immunostaining analysis revealed that Lace1 KO mice iWAT had more Ucp1 positive adipocytes than WT under cold exposure (Figure. 21 F). BAT activation is not changed between genotypes upon cold exposure (Figure. 22 C-F). Subsequently, I examined the systemic metabolic phenotype of Lace1 KO mice under cold exposure and found increased $VO_2$ (Figure. 23 A-B) and heat generation (Figure. 23 C-D) in Lace1 KO mice under cold exposure. These data suggested that Lace1 KO mice increased energy expenditure compared with littermate controls under cold conditions. Also, I found that Lace1 KO mice had higher rectal temperatures than WT under cold conditions (Figure. 24 A-B), indicating that Lace1 KO mice exhibited cold tolerance and maintained their core body temperature under cold exposure. The results suggest that Lace1 deficiency promotes iWAT browning under cold conditions.

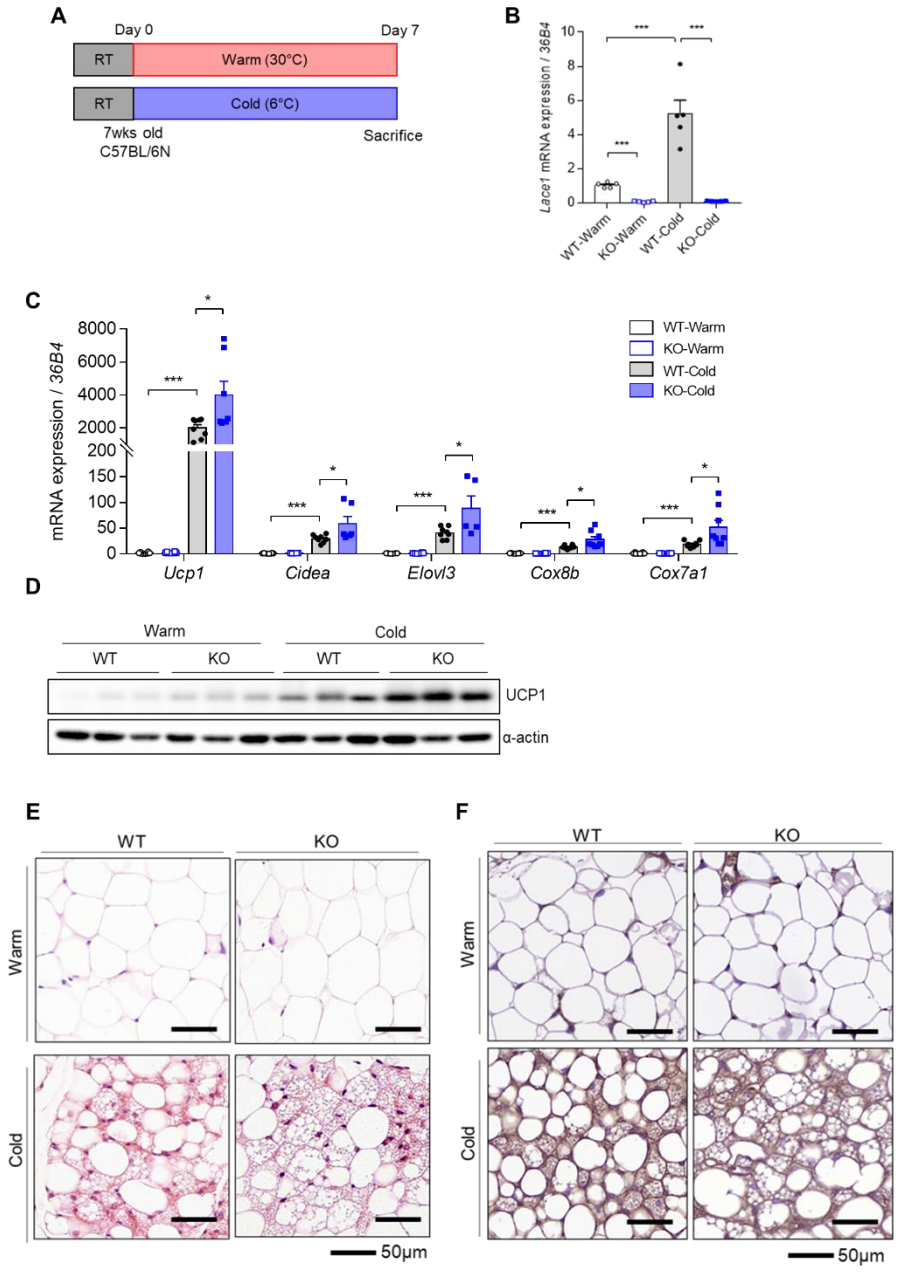


**Figure 21. Increased browning of iWAT in Lace1 KO mice upon cold exposure.**

(A) Scheme of cold exposure for 7 days. (B) *Lace1* mRNA expression in iWAT of Lace1 KO mice under cold exposure; n = 5 for all groups. (C) Thermogenesis-related gene expression in iWAT of Lace1 KO under cold exposure; n = 7 for all groups. (D) LACE1 and UCP1 protein expression in iWAT of Lace1 KO mice under cold exposure; n = 3 for all groups. (E) Representative H&E staining of iWAT in Lace1 KO mice under cold exposure (scale bar: 50 μm); n = 3 for all groups. (F) UCP1 immunohistochemistry staining of iWAT in Lace1 KO mice under cold exposure (scale bar: 50 μm); n = 3 for all groups. All experiments were performed after intervention. Values are shown as mean ± SEM. Significance calculated using unpaired two-tailed student's t-test. *$p < 0.05$, **$p < 0.01$, ***$p < 0.001$.

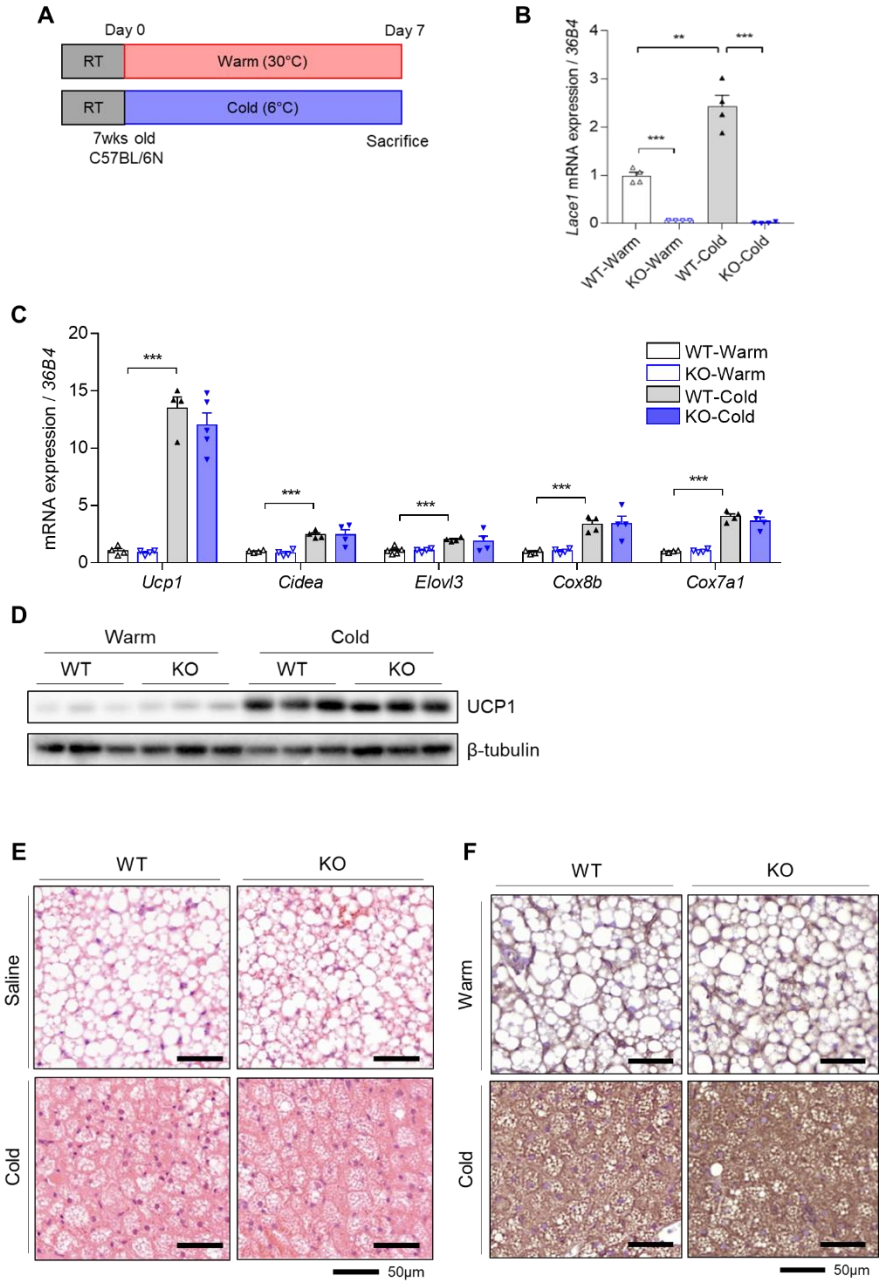


**Figure 22. BAT activation in Lace1 KO mice upon cold exposure.**

(A) Scheme of cold exposure for 7 days. (B) *Lace1* mRNA expression in BAT of Lace1 KO mice under cold exposure; n = 4 for all groups. (C) Thermogenesis-related gene expression in BAT of Lace1 KO under cold exposure; n = 4 for all groups. (D) UCP1 protein expression in BAAT of Lace1 KO mice under cold exposure; n = 3 for all groups. (E) Representative H&E staining of BAT in Lace1 KO mice under cold exposure (scale bar: 50 μm); n = 3 for all groups. (F) UCP1 immunohistochemistry staining of BAT in Lace1 KO mice under cold exposure (scale bar: 50 μm); n = 3 for all groups. All experiments were performed after intervention. Values are shown as mean ± SEM. Significance calculated using unpaired two-tailed student's t-test. *$p < 0.05$, **$p < 0.01$, ***$p < 0.001$.

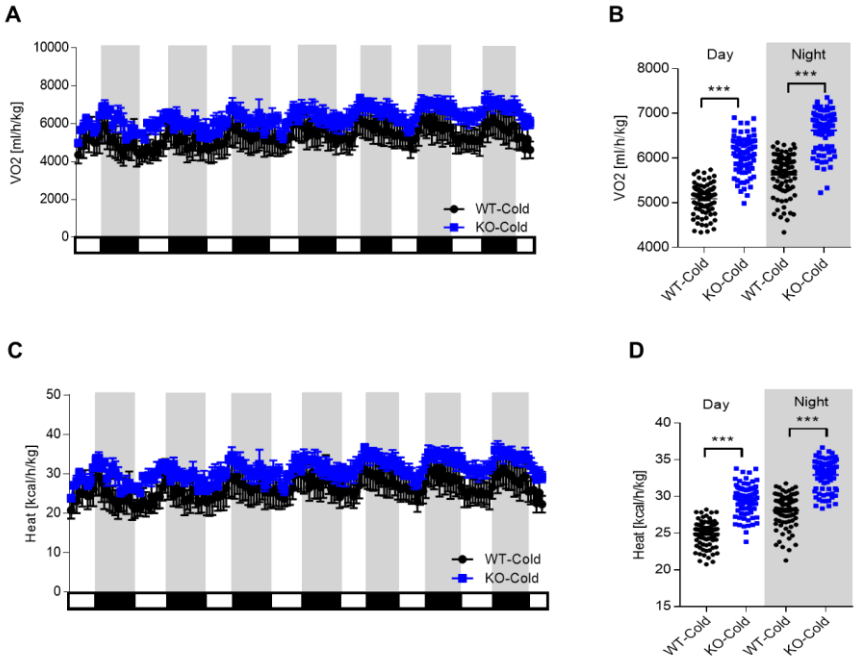


**Figure 23. Increased energy expenditure in Lace1 KO mice upon cold exposure.**

Whole-body $VO_2$ and (A-B) heat generation (C-D) in Lace1 KO upon cold exposure for 7 days; n = 5 for all groups. All experiments were performed after intervention. Values are shown as mean ± SEM. Significance calculated using unpaired two-tailed student's t-test. *p < 0.05, **p < 0.01, ***p < 0.001.

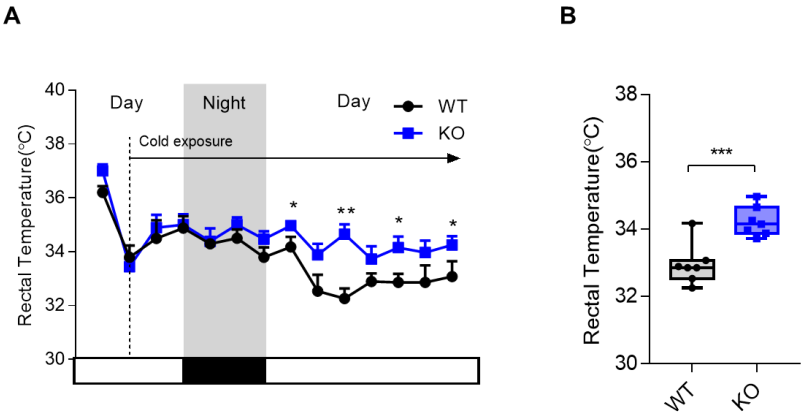


**Figure 24. The increased rectal temperature in Lace1 KO mice upon cold exposure.**

Rectal temperature under cold exposure in Lace1 KO mice; n = 8 for all groups. All experiments were performed after intervention. Values are shown as means ± SEM. Significance calculated using unpaired two-tailed student's t-test. *p < 0.05, **p < 0.01, ***p < 0.001.

**5. Lace1 deficiency results in increased iWAT browning after wheel running exercise**

Mice were performed voluntary wheel running exercise for 4-weeks to investigate the Lace1 KO mice phenotype under exercise. I found that thermogenesis-related gene level is increased in iWAT of Lace1 KO mice after wheel running exercise (Figure. 25 C). Additionally, Lace1 KO mice displayed higher UCP1 protein expression in iWAT than WT after wheel running exercise (Figure. 25 D). Histological analysis indicated that Lace1 KO mice had more beige fat than WT after wheel running exercise (Figure. 25 E). UCP1 immunostaining analysis revealed that Lace1 KO mice had more UCP1-positive adipocytes than WT after wheel running exercise (Figure. 25 F). BAT activation did not differ between WT and KO mice after wheel running exercise (Figure. 26 C-F). Also, I tried to measure rectal temperature after the onset of acute exhausted treadmill exercise for heat generation capacity analysis. Interestingly, Lace1 KO mice had higher rectal temperature than WT after the onset of exhausted exercise (Figure. 27 A).

These data indicated that Lace1 deficiency promotes browning of iWAT after wheel running exercise.

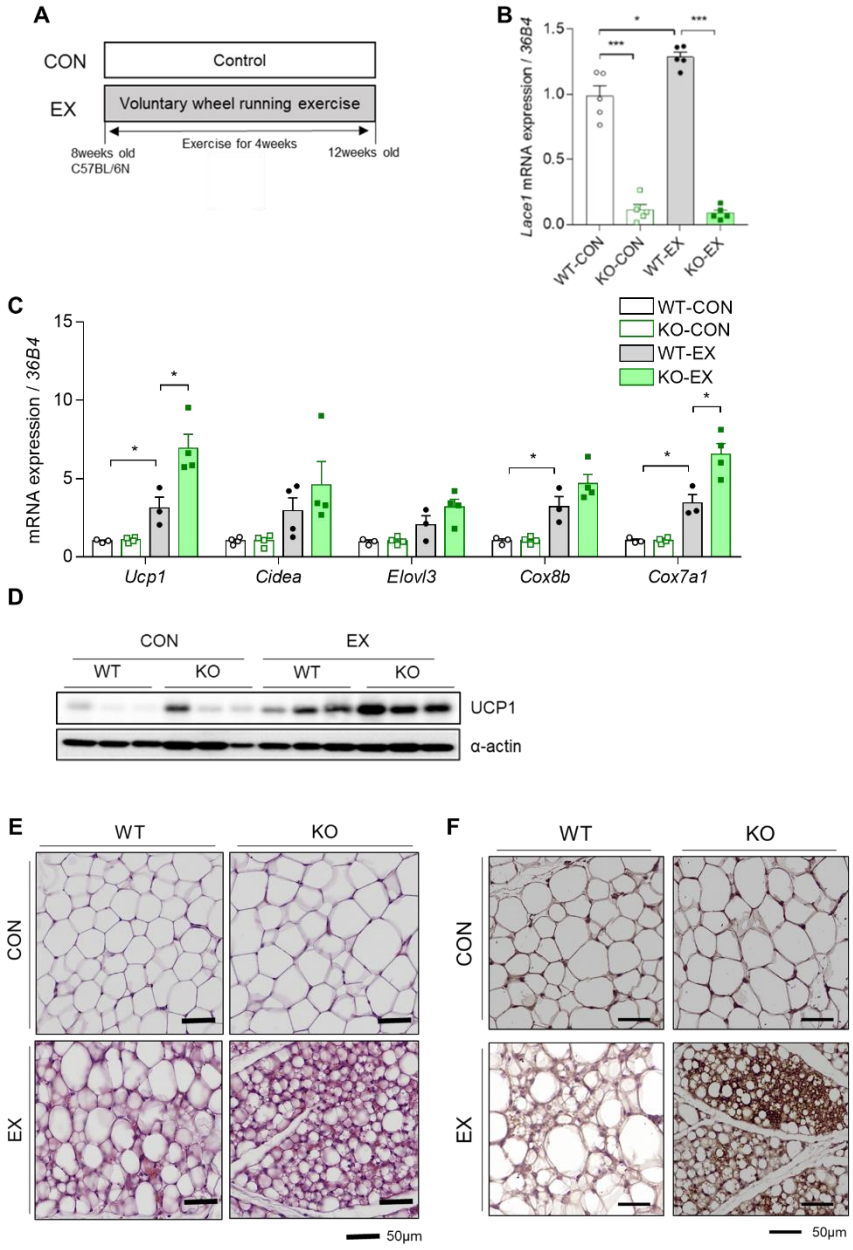


**Figure 25. Increased browning of iWAT in Lace1 KO mice after wheel running exercise.**

(A) Scheme of voluntary wheel running exercise for 4 weeks. (B) *Lace1* mRNA expression in iWAT of Lace1 KO mice after wheel running exercise; n = 5 for all groups. (C) Thermogenesis-related gene expression in iWAT of Lace1 KO after wheel running exercise; n = 7 for all groups. (D) LACE1 and UCP1 protein expression in iWAT of Lace1 KO mice after wheel running exercise; n = 3 for all groups. (E) Representative H&E staining of iWAT in Lace1 KO mice after wheel running exercise (scale bar: 50 μm); n = 3 for all groups. (F) UCP1 immunohistochemistry staining of iWAT in Lace1 KO mice after wheel running exercise (scale bar: 50 μm); n = 3 for all groups. All experiments were performed after intervention. Values are shown as mean ± SEM. Significance calculated using unpaired two-tailed student's t-test. *$p < 0.05$, **$p < 0.01$, ***$p < 0.001$

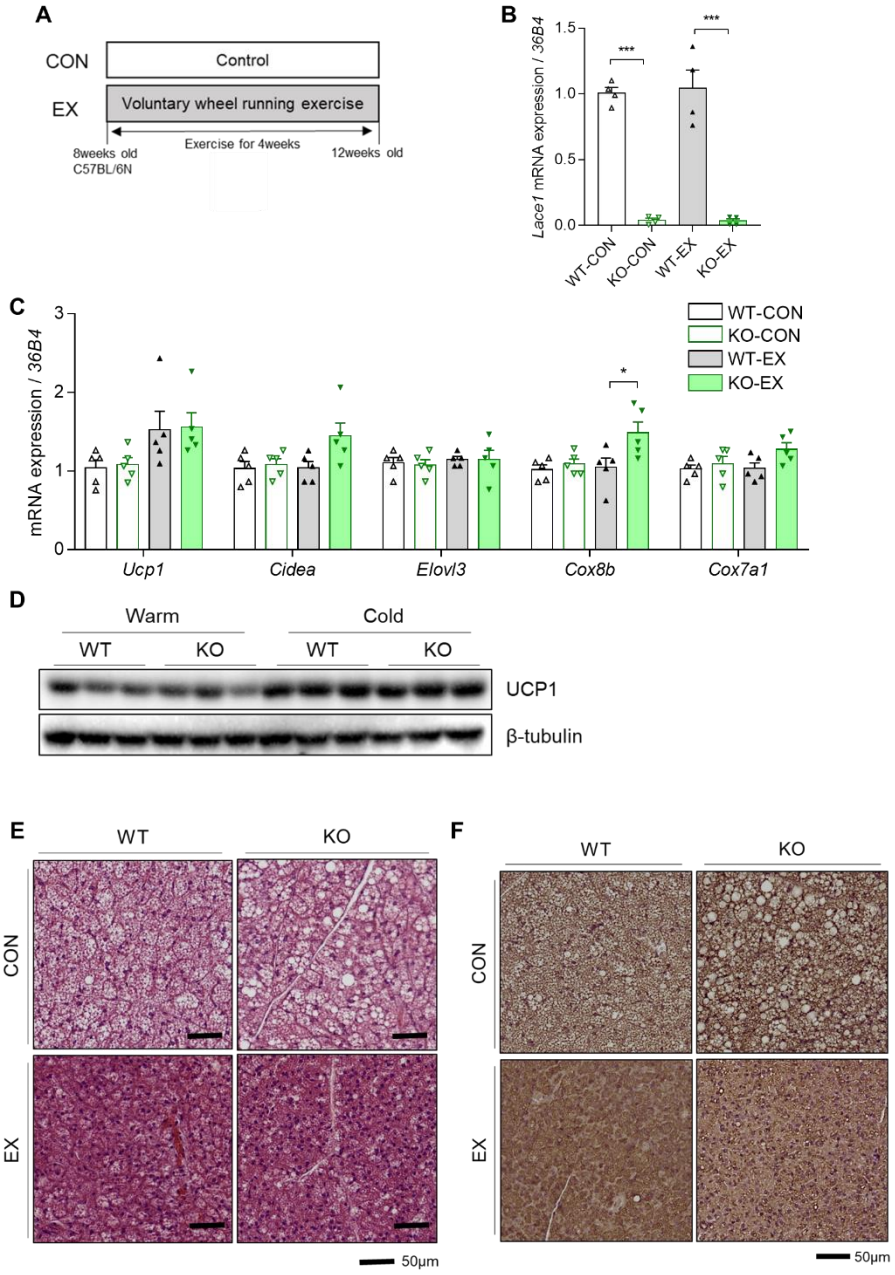


**Figure 26. BAT activation in Lace1 KO mice after aerobic exercise training.**

(A) Scheme of voluntary wheel running exercise for 4 weeks. (B) *Lace1* mRNA expression in BAT of Lace1 KO mice after wheel running exercise; n = 5 for all groups. (C) Thermogenesis-related gene expression in BAT of Lace1 KO after wheel running exercise; n = 7 for all groups. (D) LACE1 and UCP1 protein expression in BAT of Lace1 KO mice after wheel running exercise; n = 3 for all groups. (E) Representative H&E staining of BAT in Lace1 KO mice after wheel running exercise (scale bar: 50 μm); n = 3 for all groups. (F) UCP1 immunohistochemistry staining of BAT in Lace1 KO mice after wheel running exercise (scale bar: 50 μm); n = 3 for all groups. All experiments were performed after intervention. Values are shown as mean ± SEM. Significance calculated using unpaired two-tailed student's t-test. *$p < 0.05$, **$p < 0.01$, ***$p < 0.001$

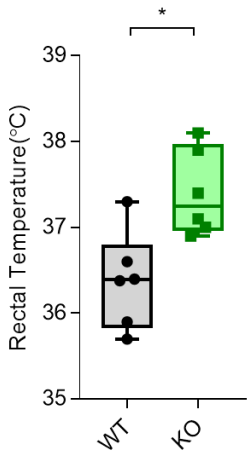


**Figure 27. Increased heat generation after onset acute exhausted exercise.** Rectal temperature after onset acute exhausted treadmill exercise of Lace1 KO mice. All experiments were performed after intervention. Values are shown as mean ± SEM. Significance calculated using unpaired two-tailed student's t-test. *p < 0.05, **p < 0.01, ***p < 0.001

**6. Lace1 loss promotes lactate/GPR81 signaling in CL-induced iWAT**

I analyzed and compared upregulated iWAT genes between WT and Lace1 KO mice under CL challenge using bulk RNA sequencing to investigate the acceleration of iWAT browning in Lace1 deficiency. The RNA-seq data suggested that the hydroxycarboxylic acid receptor1 (Hcar1) gene was more upregulated in Lace1 KO mouse iWAT under CL than in WT mice (Figure. 28 A-B). *Hcar1* is a G protein-coupled receptor 81 (Gpr81) gene that functions as a receptor for lactate (Lee et al., 2001; Roland et al., 2014). Gpr81 is expressed in adipose tissue, liver, and muscle and increased in iWAT under CL challenge (Yao et al., 2020). Therefore, I hypothesized that Lace1 KO mice exhibited higher iWAT browning capacity than WT due to lactate utilization. The receptor *Hcar1* mRNA level increased in Lace1 KO mouse iWAT compared with control littermates under CL challenge. (Figure. 29 A). L-lactate is a metabolite produced from pyruvate during anaerobic glycolysis (Brooks, 2018). Recent studies have shown that lactate metabolites are a new white adipose tissue browning factor (Carriere et al., 2014; Yao *et al.*, 2020). Therefore, I injected 7-week-old male C57BL/6N mice with L-lactate once a day for 3 days and found that it increased Ucp1 mRNA and protein expression (Figure. 29 B-D). Therefore, I speculated that the increased browning capacity in Lace1 KO mice was due to upregulated CL-induced iWAT browning via lactate/GPR81 signaling.

Subsequently, I determined monocarboxylate transporter 1 (Mct1) expression

levels to investigate iWAT lactate uptake ability in Lace1 KO mice under CL challenge. Previous studies have reported that Mct1 expression in WAT and BAT is controlled by physiological browning stimuli (De Matteis et al., 2013), indicating that lactate might regulate white adipocyte browning (Carriere *et al.*, 2014). Additionally, lactate transport through Mct1 controls Ucp1 expression in adipocytes (Yao *et al.*, 2020). First, I confirmed that the Mct1 mRNA and protein level increased in iWAT of Lace1 KO mice under CL challenge (Figure. 30 A-B). However, the lactate efflux transporter, monocarboxylate transporter 4 (*Mct4*) mRNA level did not change in iWAT of Lace1 KO mice under CL challenge (Figure. 1-30 A).

Lactate can be converted to pyruvate to increase Ucp1 expression using lactate dehydrogenase (LDH) in iWAT and BAT (Carriere *et al.*, 2014). Lactate dehydrogenase B (Ldhb) converts lactate to pyruvate; conversely, lactate dehydrogenase A (Ldha) converts pyruvate to lactate (Urbanska and Orzechowski, 2019). I then determined *Ldhb* and *Ldha* mRNA expression in iWAT under CL challenge and found that Lace1 KO increased *Ldhb* mRNA expression but did not change *Ldha* mRNA expression under CL challenge compared with control littermates (Figure. 31 A). Additionally, the Ldhb/Ldha ratio increased in Lace1 KO mice under CL (Figure. 31 B).

Next, I analyzed *Mct1* mRNA levels in whole tissue of Lace1 KO mice under CL challenge and found that it only increased in iWAT of Lace1 KO mice under CL challenge, but did not change in other tissues (Figure. 32 A). These results

indicated that Lace1-deficient mice promoted lactate uptake in iWAT compared to control littermates under CL challenge. These findings revealed that lactate-induced iWAT browning increased in Lace1-deficient mice compared with WT.

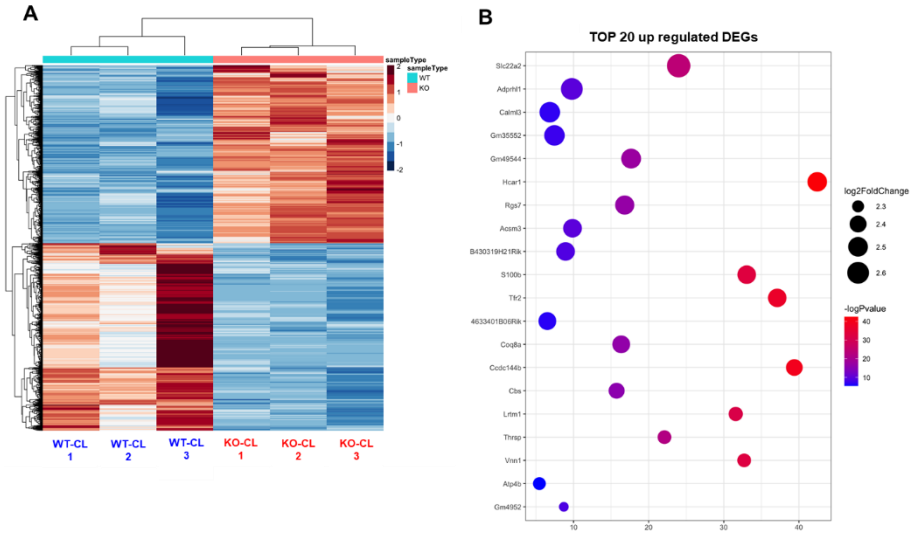


**Figure 28. Transcriptomic analysis of iWAT in Lace1 KO mice upon CL injection.**

(A) Heat map of iWAT in Lace1 KO mice upon CL-316,243 challenge; n=3 for all group. (B) Top 20 upregulated differentially expressed genes (DEGs) of iWAT in Lace1 KO mice compared with WT mice under CL challenge. All experiments were performed after intervention. Values are shown as mean ± SEM. Significance calculated using unpaired two-tailed student's t-test.

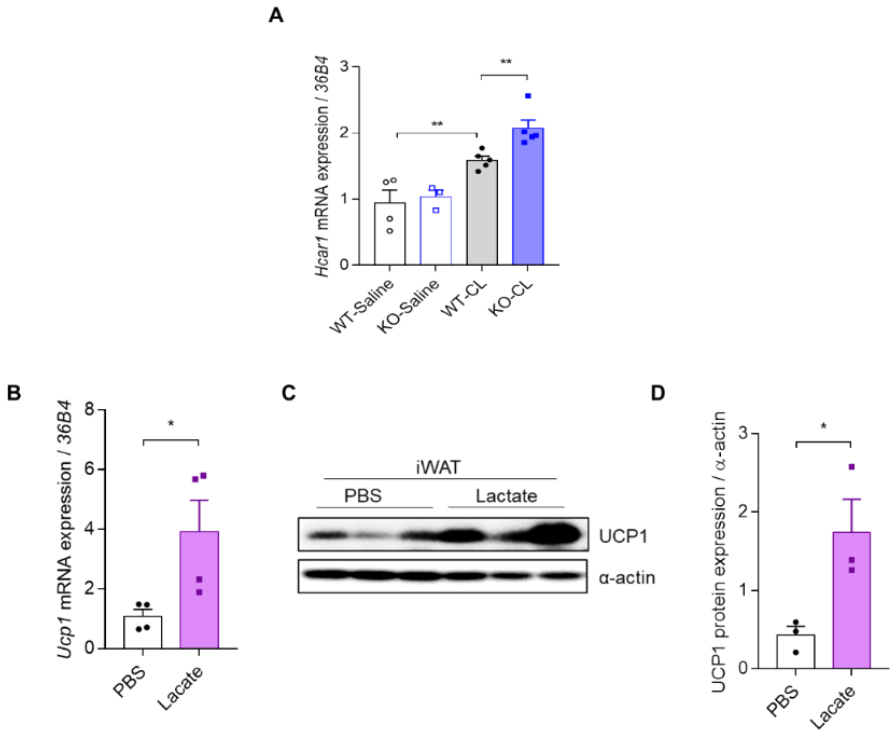


**Figure 29. Lactate induced browning in iWAT.**

(A) *Hcar1* mRNA expression in iWAT of Lace1 KO mice under CL challenge; n = 5 for all groups. (B) *Ucp1* mRNA level under L-lactate injection; n = 4 for all groups. (C-D) UCP1 protein level under L-lactate injection; n = 3 for all groups. Protein expression is quantified by α-actin expression level. All experiments were performed after intervention. Values are shown as mean ± SEM. Significance calculated using unpaired two-tailed student's t-test. *p < 0.05, **p < 0.01, ***p < 0.001.

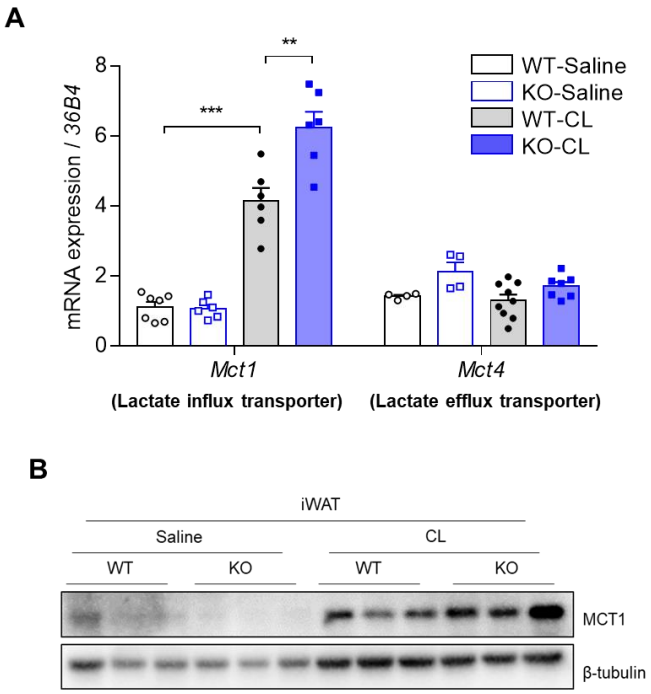


**Figure 30. Increased browning of iWAT in Lace1 KO mice by lactate uptake and utilization.**

(A) *Mct1* and *Mct4* mRNA expression in iWAT of Lace1 KO mice under CL challenge. WT-Saline, n = 7; KO-Saline, n = 6; WT-CL, n = 6; KO-CL, n = 6. (B) MCT1 protein levels in iWAT of Lace1 KO mice under CL challenge; n = 3 for all groups. All experiments were performed after intervention. Values are shown as mean ± SEM. Significance calculated using unpaired two-tailed student's t-test. *p < 0.05, **p < 0.01, ***p < 0.001.

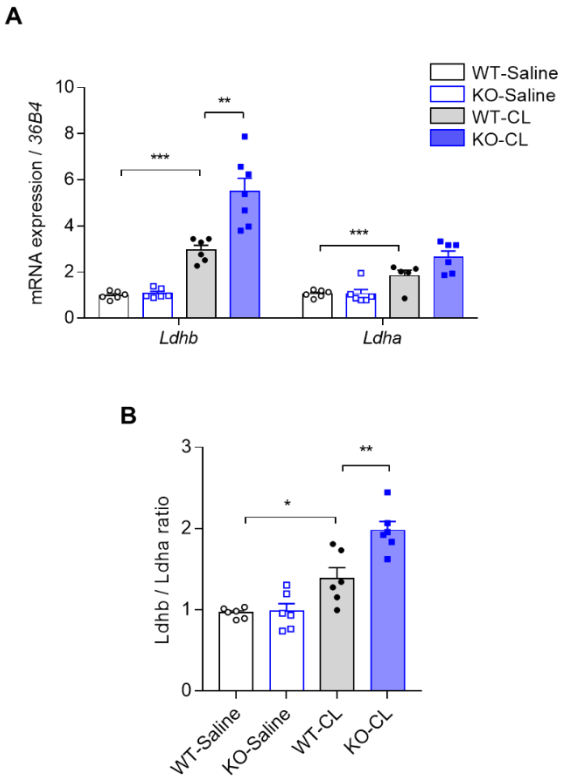


**Figure 31. Increased LDH activity of iWAT in Lace1 KO mice.**

(A) *Ldhb* and *Ldha* mRNA expression in iWAT of Lace1 KO mice under CL challenge; n = 5 for all group. WT-Saline, n = 6; KO-Saline, n = 6; WT-CL, n = 6; KO-CL, n = 7. (B) Ldhb/Ldha expression ratio in iWAT of Lace1 KO mice under CL challenge. Values were calculated using mRNA expression values; n = 5 for all groups. WT-Saline, n = 6; KO-Saline, n = 6; WT-CL, n = 6; KO-CL, n = 7. All experiments were performed after intervention. Values are shown as means ± SEM. Significance calculated using unpaired two-tailed student's t-test. *$p < 0.05$, **$p < 0.01$, ***$p < 0.001$.

**7. Loss of Lace1 results in inactivation of pyruvate dehydrogenase to promote lactate efflux in CL-induced heart**

To investigate the much higher circulating L-lactate levels in Lace1 KO compared to control littermates, I determined *Mct4* mRNA expression in whole tissue of Lace1 KO mice under CL challenge and found that it was only increased in heart of Lace1 KO mice than in control littermates (Figure. 32 B). Based on the increased *Mct4* mRNA levels in the heart tissue of Lace1 KO mice under CL challenge, I hypothesized that lactate released from heart tissue contributed to lactate uptake and utilization in the browning process of iWAT in Lace1 KO mice under CL challenge.

Lactate release through Mct4 activation in heart tissue is a cardiac hypertrophy phenotype (Cluntun et al., 2021) that may proceed to heart failure by increasing cardiomyocytes and heart size. (Cluntun *et al.*, 2021; Zhu et al., 2013). However, hypertrophic morphology was not observed in the heart tissue of Lace1 KO mice under CL challenge (Figure. 33 A). Interestingly, I found that hypertrophy-related gene expression is increased in heart of Lace1 KO mice under CL challenge (Figure. 33 B). It is well established that cardiac hypertrophy is induced by cardiac hypoxia (Rajinikanth Gogiraju et al. 2019). Therefore, I tried to confirm HIF1α protein expression which is a representative marker of hypoxia. Interestingly, I found that HIF1α protein expression tends to be increased in heart of Lace1 KO mice upon CL challenge (Figure. 33 C-D).

Also, I found that the heart tissue of Lace1 KO mice exhibited greater pyruvate dehydrogenase (PDH) inactivation than WT under CL challenge (Figure. 34 B-C). When PDH is inactivated, pyruvate from glycolysis cannot be converted to acetyl CoA; therefore, it is converted to lactate, and the unbalanced pyruvate-lactate axis releases lactate into the blood (Cluntun *et al.*, 2021). Additionally, Ldha mRNA and protein levels (Figure. 35 A-B) and Mct4 mRNA and protein expression levels (Figure. 36 A-B) were increased in the heart tissue of Lace1 KO mice under CL challenge compared with control littermates. In line with this, I measured serum L-lactate and found that circulating L-lactate was increased in Lace1 KO mice compared with control littermates under CL challenge (Figure. 36 C).

These findings indicated that lactate-induced browning was enhanced in iWAT due to increased lactate efflux by PDH phosphorylation in the heart tissue of Lace1 KO mice under CL challenge.

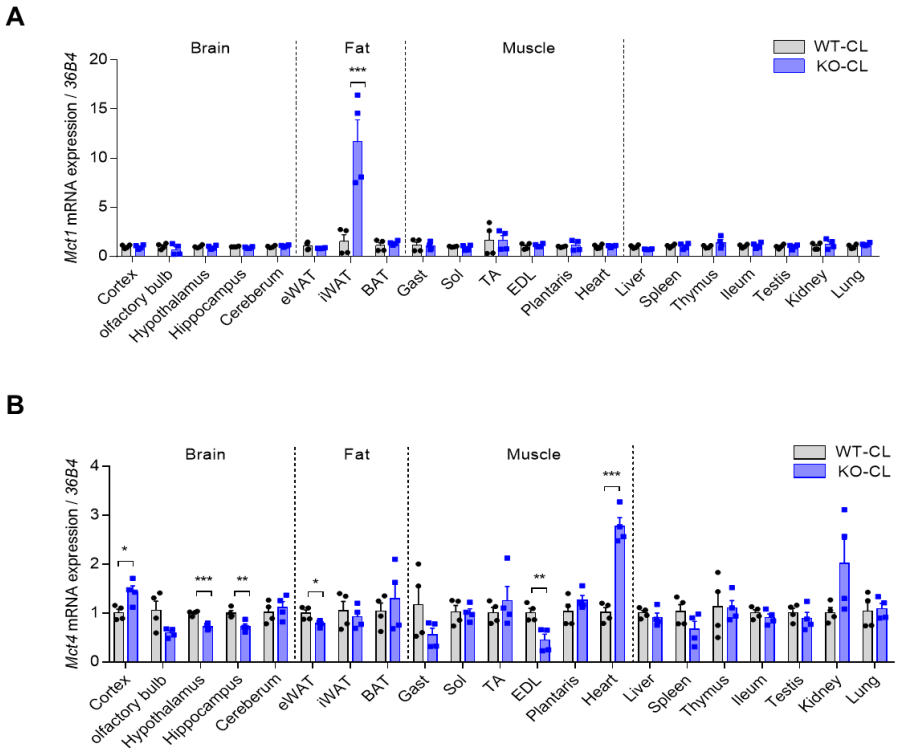


**Figure 32. *Mct1* and *Mct4* mRNA level of whole tissue in Lace1 KO mice under CL challenge.**

(A) *Mct1* mRNA levels in whole tissue of Lace1 KO mice under CL challenge; n = 4 for all groups. (B) *Mct4* mRNA levels in whole tissue of Lace1 KO mice under CL challenge; n = 4 for all groups. All experiments were performed after intervention. Values are shown as mean ± SEM. Significance calculated using unpaired two-tailed student's t-test. *$p < 0.05$, **$p < 0.01$, ***$p < 0.001$.

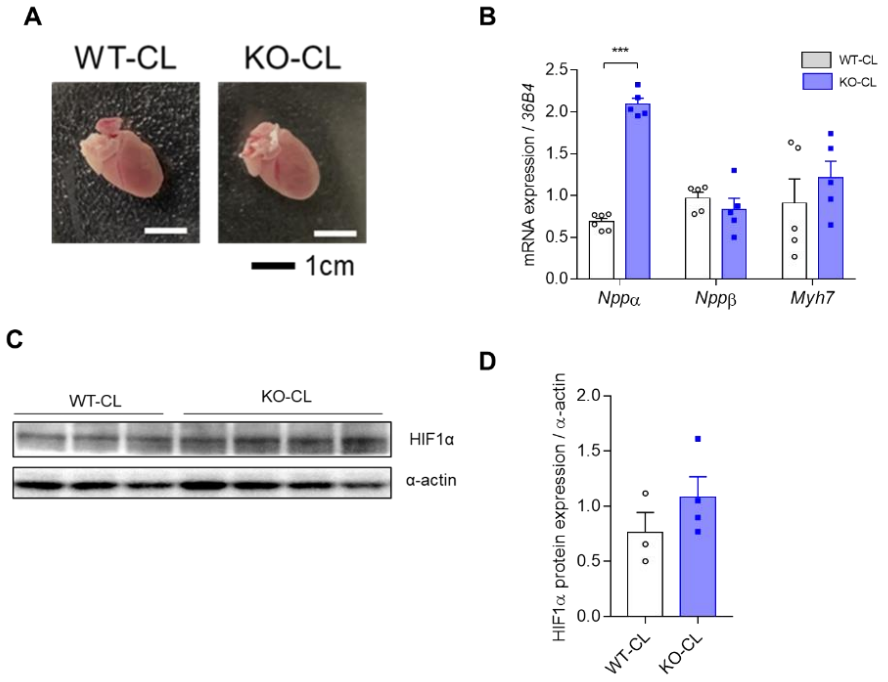


**Figure 33. Cardiac hypertrophy related gene expression in Lace1 KO mice.**

(A) Representative image of the heart in Lace1 KO mice upon CL-316,243 challenge; n=3 for all group. (B) Hypertrophy-related gene expression level of the heart in Lace1 KO mice upon CL-316,243 challenge; n=5 for all group. (C-D) HIF1α protein expression of the heart in Lace1 KO mice upon CL-316,243 challenge. WT-CL; n=3, KO-CL; n=4. Protein expression level quantified by α-actin expression. Values are shown as means ± SEM. Significance calculated using unpaired two-tailed student's t-test. *$p < 0.05$, **$p < 0.01$, ***$p < 0.001$.

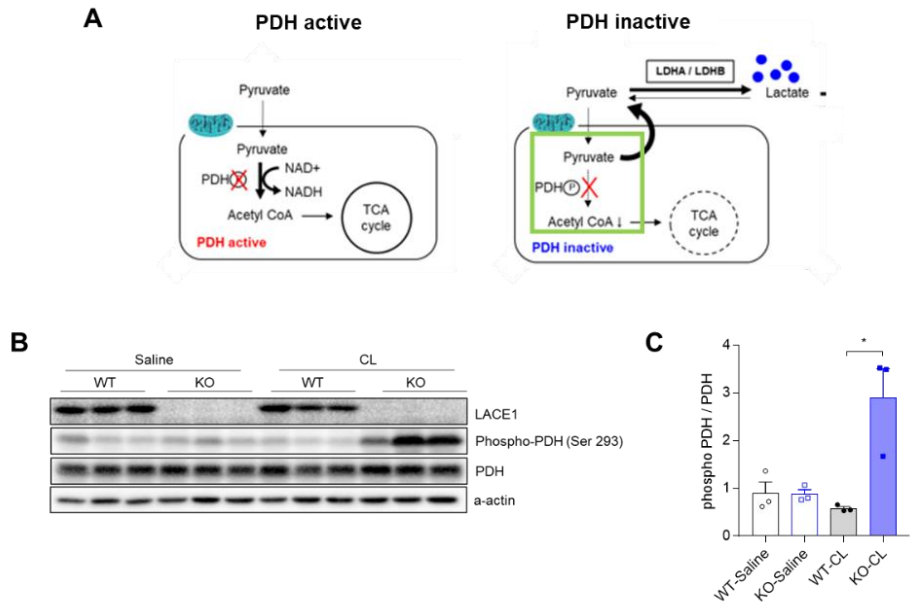


**Figure 34. Phosphorylation of PDH of heart in Lace1 KO mice upon CL challenge.**

(A) Mechanisms of lactate release via PDH phosphorylation. (B-C) Lace1, phospho-PDH (Ser 293), and total PDH protein levels in heart tissue of Lace1 KO mice under CL challenge. Protein expression level quantified by α-actin level; n = 3 for all groups. All experiments were performed after intervention. Values are shown as mean ± SEM. Significance calculated using unpaired two-tailed student's t-test. *$p < 0.05$, **$p < 0.01$, ***$p < 0.001$.

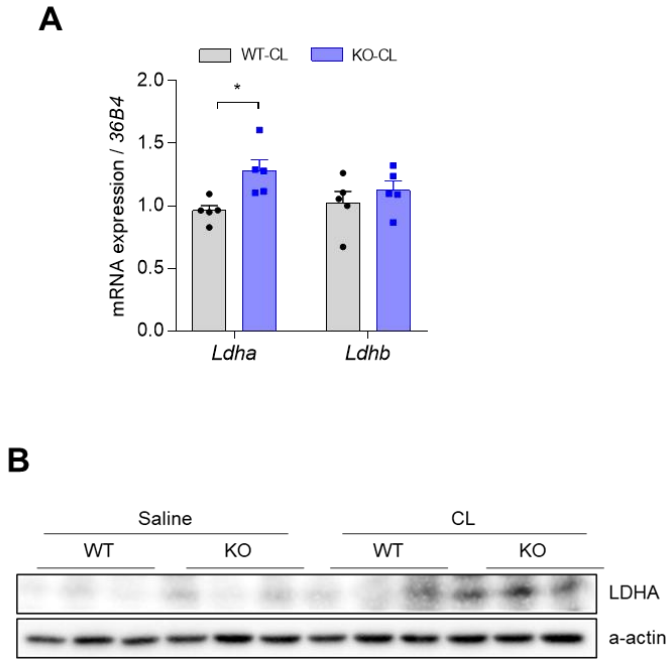


**Figure 35. LDH activity of the heart in Lace1 KO mice upon CL challenge.** (A) *Ldha* and *Ldhb* mRNA expression in heart tissue of Lace1 KO mice under CL challenge; n = 5 for all groups. (B) LDHA protein levels in heart tissue of Lace1 KO mice under CL challenge; n = 3 for all groups. Protein expression level quantified by α-actin level; n = 3 for all groups. All experiments were performed after intervention. Values are shown as mean ± SEM. Significance calculated using unpaired two-tailed student's t-test. *p < 0.05, **p < 0.01, ***p < 0.001.

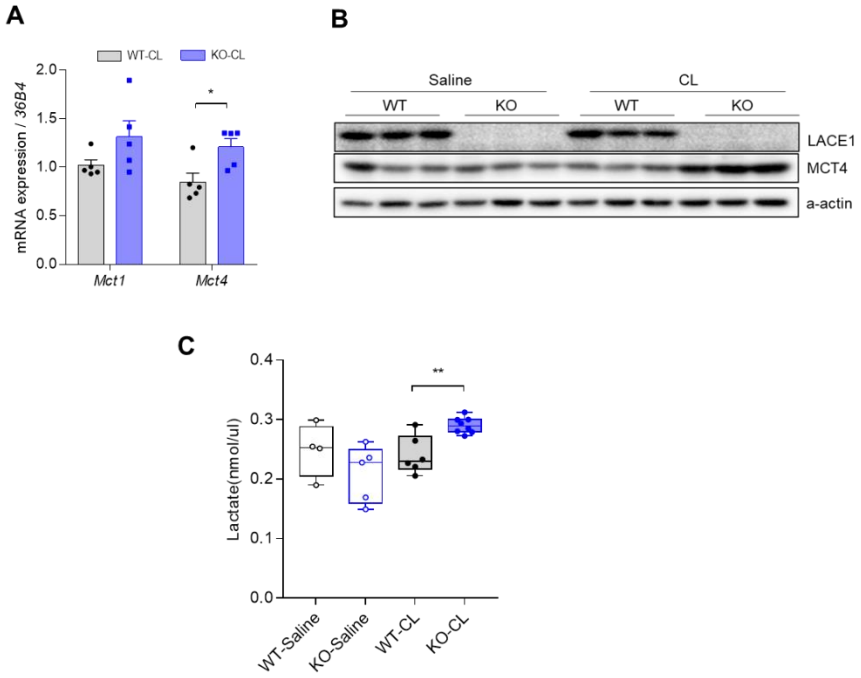


**Figure 36. Loss of Lace1 results in the inactivation of pyruvate dehydrogenase promotes lactate efflux in CL-induced heart.**

(A) *Mct1* and *Mct4* mRNA expression in heart tissue of Lace1 KO mice under CL challenge; n = 5 for all groups. (B) LACE1 and MCT4 protein levels in heart tissue of Lace1 KO mice under CL challenge; n = 3 for all groups. Protein expression level quantified by α-actin level; n = 3 for all groups. (C) Serum L-lactate amounts (nM/μl) in Lace1 KO mice under CL challenge. WT-Saline; n=4, KO-Saline; n=5, WT-CL; n=6, KO-CL; n=8. All experiments were performed after intervention. Values are shown as mean ± SEM. Significance calculated using unpaired two-tailed student's t-test. *$p < 0.05$, **$p < 0.01$, ***$p < 0.001$.

# DISCUSSION

This study examined the role of Lace1 in iWAT browning. Lace1 expression was greatly increased in iWAT by browning stimuli such as CL injection and cold exposure. However, the browning capacity of Lace1-deficient mice was not reduced; rather, they also showed high browning capacity. To understand these conflicting findings, I investigated the mechanisms by which Lace1-deficient mice enhance browning capacity and found that CL-induced browning upregulation in Lace1-deficient mice was stimulated by lactate uptake in iWAT, suggesting for the first time that this phenomenon was due to increased lactate secretion induced by PDH phosphorylation in the heart tissue of Lace1 KO mice.

First, my data revealed that the expression of Lace1 in the iWAT browning process under CL stimulation and cold exposure was significantly correlated with Ucp1 levels. Ucp1 is the most representative adipose tissue browning marker and is dominantly expressed in cells with many mitochondria, such as BAT (Harms and Seale, 2013; Kajimura and Saito, 2014). Thus, there is accumulating evidence of the Ucp1 expression mechanism in brown and beige adipocytes with high mitochondrial content and its effect on whole-body energy homeostasis. Therefore, I have provisionally concluded that the Lace1 gene plays an important role in the browning process.

β3-ARs are the predominant WAT browning regulators, and CL is a potent and highly selective β3-AR agonist (Grujic et al., 1997). Several studies on WAT browning have reported that CL treatment significantly increased browning marker-gene expression, reduced lipid droplet size, and increased heat generation and energy expenditure in BAT and iWAT (Cero et al., 2021) (Xiao et al., 2015), becoming more evident over time. Since I identified Lace1 as an important gene in browning, I stimulated CL in Lace1 KO mice to determine the effects of Lace1 on the browning process and found that Lace1 KO mice had smaller lipid droplets and higher Ucp1 expression following CL treatment. Furthermore, the oxygen uptake capacity and heat generation were significantly higher in KO mice than in control littermates. Cold exposure had a similar effect.

To better understand these results, I performed RNA-seq to investigate which gene expressions were altered in CL-induced iWAT in Lace1 KO mice and found that Hcar1 gene expression was the highest. This finding led us to establish a new hypothesis. Hcar1, also known as GPR81, is a cell-surface receptor for lactate and is highly expressed in adipose tissue and found in the kidney, skeletal muscles, and the liver in mammals (Yao *et al.*, 2020). Lactate-induced GPR81 effectively suppresses lipolysis via modulation of the cyclic adenosine monophosphate (cAMP)-PKA pathway and contributes to HSL downregulation in adipose tissue (Cai et al., 2008; Ge et al., 2008). Furthermore,

activation of the GPR 81-induced cAMP-PKA pathway-dependent anti-lipolytic effect acted synergistically with insulin (Langin, 2010). These results suggest that lactate can modulate metabolic processes in adipose tissue by Gpr81-dependent mechanisms.

Lactate metabolites contribute to browning. Recent studies have reported that lactate plays a crucial role in the WAT browning through its receptor GPR81 and transporter Mct1 in a β3-AR stimulation-dependent manner (Lagarde et al., 2021; Yao *et al.*, 2020). Based on my RNA-seq data and the results of a previous study, I hypothesized that CL-induced Hcar1 gene expression in iWAT of Lace1 KO mice could be due to increased circulating lactate levels. Serum lactate significantly increased in CL-induced Lace1 KO mice compared with WT mice, and its receptor *Hcar1* mRNA levels were also significantly elevated in Lace KO mice. Additionally, I confirmed the lactate uptake ability of Lace1 KO mice by CL stimulation and found that Mct1, a lactate influx transporter, was specifically expressed only in iWAT. Lagarde et al. reported a positive correlation between Mct1 and thermogenic marker-gene levels in iWAT. These findings showed that Ucp1-positive cells were highly detected in the subpopulation of adipocytes expressing Mct1 after cold exposure. Lactate is first converted to pyruvate by the LDH oxidation reaction, indicating that lactate consumption is directly dependent on mitochondrial pyruvate utilization (Brooks, 2018; Glancy et al., 2021). CL-induced Lace1 KO mice displayed

significantly elevated Ldhb expression levels in iWAT compared to WT mice. These results suggested that CL-stimulated WAT of Lace1 KO mice uptook more lactate via Mct1 upregulation than WT mice and increased Ucp1 expression by increasing oxidative phosphorylation in mitochondria by a high rate of conversion to pyruvate. These findings are important in discussions on the role of lactate in β3-AR-induced iWAT browning.

Although Lace1 KO mice displayed a higher browning capacity through lactate uptake under CL stimulation, lactate concentrations in iWAT did not differ between WT and KO mice. Therefore, to determine the reason for lactate increase, I measured Mct4, a lactate exporter, in whole tissue of CL-stimulated WT and KO mice using the same concept as Mct1 in iWAT. Notably, in contrast to the Mct1 results of iWAT, CL-induced Lace1 KO mice exclusively induced increased Mct4 expression in heart tissue compared with WT mice. Under normal conditions, cardiomyocytes express low levels of Mct4 that are increased by hypertrophy or heart failure (Cluntun *et al.*, 2021; Zhu *et al.*, 2013). However, I did not find hypertrophic morphology in CL-induced Lace1 KO mice. Unlike in previous reports, elevated Mct4 did not change the cardiac hypertrophic phenotype. Nevertheless, I noted that PDH phosphorylation was significantly increased only in Lace1 KO mice under CL treatment. PDH is the rate-limiting enzyme for glucose oxidation, and cardiac-specific PDH deletion impairs glucose oxidation in mice (Gopal et al., 2018). My results demonstrated

that increased Mct4 in CL-induced Lace1 KO mice was due to the impaired pyruvate flux into mitochondria due to PDH phosphorylation. The role of β3-ARs in heart tissue has long been debated. This receptor could represent either a protective or detrimental effect on the heart (Arioglu-Inan et al., 2019; Moniotte and Balligand, 2002). However, no studies on the effects of CL-specific β3-AR activation on heart tissue have been conducted, which was a limitation to the discussions in this study.

Ikeda et al. suggested two important reasons for beige-fat studies. First, beige fat is a unique model for understanding the effects of environmental factors on cell maintenance and fate. Second, it is important in adult humans and could be a therapeutic target in treating metabolic disorders (Ikeda et al., 2018). I first suggested that Lace1 is a new gene that regulates the browning of white adipose tissue, the main target tissue of obesity metabolism research. Furthermore, I first suggested that CL, a specific β3-AR agonist, which I used as a representative tool in browning research, regulated the browning of white fat by modulating the molecular and physiological functions of heart tissue through the Lace1 gene. Therefore, the Lace1 gene could play an important role as a therapeutic target in the study of adipose tissue browning, obesity, and metabolism.

# CONCLUSION

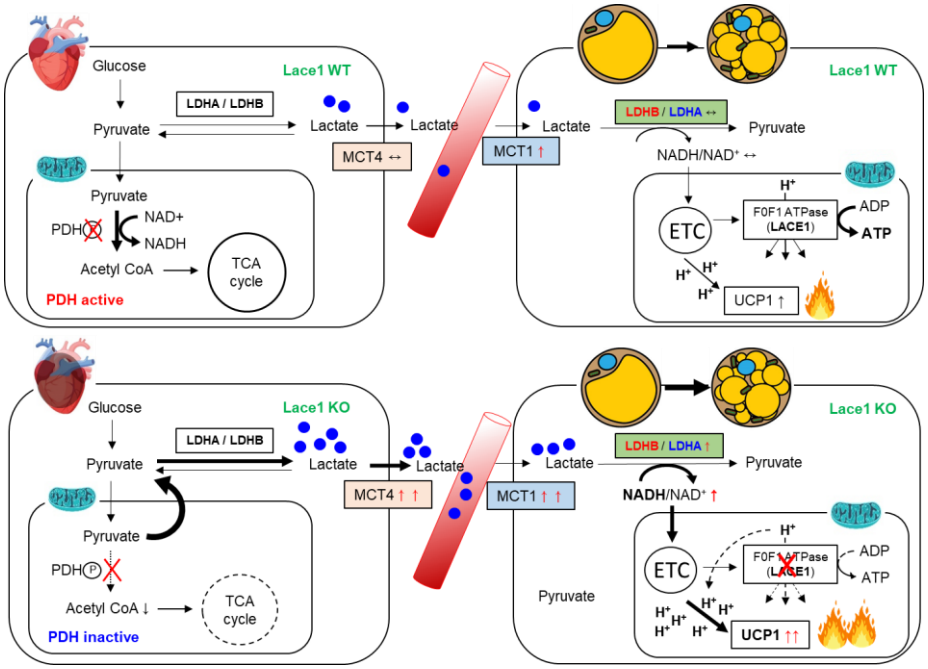
Glucose
Lace1 WT
LDHA / LDHB
Pyruvate
Lactate
Lactate
MCT4 ↔
MCT1 ↑
Lactate
LDHB / LDHA ↔
Pyruvate
NADH/NAD⁺ ↔
Pyruvate
PDH
NAD+
NADH
Acetyl CoA
TCA cycle
PDH active
H⁺
ETC
F0F1 ATPase (LACE1)
ADP
ATP
H⁺
H⁺
H⁺
UCP1 ↑
Glucose
Lace1 KO
LDHA / LDHB
Pyruvate
Lactate
Lactate
MCT4 ↑ ↑
MCT1 ↑ ↑
Lactate
LDHB / LDHA ↑
Pyruvate
NADH/NAD⁺ ↑
Pyruvate
PDH
Acetyl CoA ↓
TCA cycle
PDH inactive
Pyruvate
H⁺
ETC
F0F1 ATPase (LACE1)
ADP
ATP
H⁺ H⁺
H⁺ H⁺ H⁺
UCP1 ↑↑

This study showed that Lace1 is increased in iWAT by browning stimuli such as CL challenge, cold exposure, and wheel running exercise training. Also, I found that Lace1 is up-regulated during brown adipogenesis and beige adipogenesis. However, the browning capacity of Lace1 deficient mice was not blunted, surprisingly, accelerated by browning stimuli. To investigate why browning of iWAT is promoted in Lace1 deficient mice, I performed bulk-RNA sequencing in iWAT of Lace1 KO mice under CL challenge compared to WT. I found that *Hcar1* gene expression was highest in iWAT of Lace1 KO mice. Hcar1, also known as Gpr81, is well known as a lactate receptor. *Hcar1* is highly expressed in adipose tissue and its activation promotes adipose browning. These results suggest that lactate modulates browning process Hcar1-dependent mechanisms. Recent studies reported that lactate is a metabolite contributing to inducing WAT browning in a β-AR-dependent manner.

Based on these results, I confirmed increased lactate uptake and lactate utilization in iWAT of Lace1 KO mice upon CL challenge. Additionally, I found that Lace1 KO mice displayed a tendency to cardiac hypertrophy and PDH inactivation in heart tissue. It is well established that PDH inactivation impairs pyruvate flux into mitochondria. Accordingly, I confirmed that Lace1 KO mice increased Ldha, an enzyme that converts pyruvate to lactate, and mct4, which functions to release lactate into the blood.

I first suggested that Lace1 is a novel gene that regulates browning process in iWAT. Furthermore, these findings indicated that lactate induced browning

by modulating PDH inactivation of the heart through Lace1 deletion mouse model.

# REFERENCES

Aldiss, P., Dellschaft, N., Sacks, H., Budge, H., and Symonds, M.E. (2017). Beyond obesity - thermogenic adipocytes and cardiometabolic health. Horm Mol Biol Clin Investig *31*.

Arboix, A. (2015). Cardiovascular risk factors for acute stroke: Risk profiles in the different subtypes of ischemic stroke. World J Clin Cases *3*, 418-429.

Arioglu-Inan, E., Kayki-Mutlu, G., and Michel, M.C. (2019). Cardiac beta3 - adrenoceptors-A role in human pathophysiology? Br J Pharmacol *176*, 2482-2495.

Aune, U.L., Ruiz, L., and Kajimura, S. (2013). Isolation and differentiation of stromal vascular cells to beige/brite cells. J Vis Exp.

Balasubramanian, P., Hall, D., and Subramanian, M. (2019). Sympathetic nervous system as a target for aging and obesity-related cardiovascular diseases. Geroscience *41*, 13-24.

Bargut, T.C.L., Souza-Mello, V., Aguila, M.B., and Mandarim-de-Lacerda, C.A. (2017). Browning of white adipose tissue: lessons from experimental models. Horm Mol Biol Clin Investig *31*.

Berry, D.C., Jiang, Y., Arpke, R.W., Close, E.L., Uchida, A., Reading, D., Berglund, E.D., Kyba, M., and Graff, J.M. (2017). Cellular Aging Contributes to Failure of Cold-Induced Beige Adipocyte Formation in Old Mice and Humans. Cell Metab *25*, 166-181.

Brooks, G.A. (2018). The Science and Translation of Lactate Shuttle Theory. Cell Metab *27*, 757-785.

Cai, T.Q., Ren, N., Jin, L., Cheng, K., Kash, S., Chen, R., Wright, S.D., Taggart, A.K., and Waters, M.G. (2008). Role of GPR81 in lactate-mediated reduction of adipose lipolysis. Biochem Biophys Res Commun *377*, 987-991.

Carriere, A., Jeanson, Y., Berger-Muller, S., Andre, M., Chenouard, V., Arnaud, E., Barreau, C., Walther, R., Galinier, A., Wdziekonski, B., et al. (2014). Browning of white adipose cells by intermediate metabolites: an adaptive mechanism to alleviate redox pressure. Diabetes *63*, 3253-3265.

Cero, C., Lea, H.J., Zhu, K.Y., Shamsi, F., Tseng, Y.H., and Cypess, A.M. (2021). beta3-Adrenergic receptors regulate human brown/beige adipocyte lipolysis and thermogenesis. JCI Insight *6*.

Cesnekova, J., Rodinova, M., Hansikova, H., Houstek, J., Zeman, J., and Stiburek, L. (2016). The mammalian homologue of yeast Afg1 ATPase (lactation elevated 1) mediates degradation of nuclear-encoded complex IV subunits. Biochem J *473*, 797-804.

Chartoumpekis, D.V., Habeos, I.G., Ziros, P.G., Psyrogiannis, A.I., Kyriazopoulou, V.E., and Papavassiliou, A.G. (2011). Brown adipose tissue responds to cold and adrenergic stimulation by induction of FGF21. Mol Med *17*, 736-740.

Chechi, K., van Marken Lichtenbelt, W., and Richard, D. (2018). Brown and beige adipose tissues: phenotype and metabolic potential in mice and men. J Appl Physiol (1985) *124*, 482-496.

Cheng, S., Fernandes, V.R., Bluemke, D.A., McClelland, R.L., Kronmal, R.A., and Lima, J.A. (2009). Age-related left ventricular remodeling and associated risk for cardiovascular outcomes: the Multi-Ethnic Study of Atherosclerosis. Circ Cardiovasc Imaging *2*, 191-198.

Cluntun, A.A., Badolia, R., Lettlova, S., Parnell, K.M., Shankar, T.S., Diakos, N.A., Olson, K.A., Taleb, I., Tatum, S.M., Berg, J.A., et al. (2021). The pyruvate-lactate axis modulates cardiac hypertrophy and heart failure. Cell Metab *33*, 629-648 e610.

Cohen, P., and Spiegelman, B.M. (2015). Brown and Beige Fat: Molecular Parts of a Thermogenic Machine. Diabetes *64*, 2346-2351.

Contreras-Baeza, Y., Sandoval, P.Y., Alarcon, R., Galaz, A., Cortes-Molina, F., Alegria, K., Baeza-Lehnert, F., Arce-Molina, R., Guequen, A., Flores, C.A., et al. (2019). Monocarboxylate transporter 4 (MCT4) is a high affinity transporter capable of exporting lactate in high-lactate microenvironments. J Biol Chem *294*, 20135-20147.

Cuspidi, C., Negri, F., Sala, C., Valerio, C., and Mancia, G. (2012). Association of left atrial enlargement with left ventricular hypertrophy and diastolic dysfunction: a tissue Doppler study in echocardiographic practice. Blood Press *21*, 24-30.

Cypess, A.M., and Kahn, C.R. (2010). The role and importance of brown adipose tissue in energy homeostasis. Curr Opin Pediatr *22*, 478-484.

De Matteis, R., Lucertini, F., Guescini, M., Polidori, E., Zeppa, S., Stocchi, V., Cinti, S., and Cuppini, R. (2013). Exercise as a new physiological stimulus for

brown adipose tissue activity. Nutr Metab Cardiovasc Dis *23*, 582-590.

Ge, H., Weiszmann, J., Reagan, J.D., Gupte, J., Baribault, H., Gyuris, T., Chen, J.L., Tian, H., and Li, Y. (2008). Elucidation of signaling and functional activities of an orphan GPCR, GPR81. J Lipid Res *49*, 797-803.

Gerdts, E., Roman, M.J., Palmieri, V., Wachtell, K., Smith, G., Nieminen, M.S., Dahlof, B., and Devereux, R.B. (2004). Impact of age on left ventricular hypertrophy regression during antihypertensive treatment with losartan or atenolol (the LIFE study). J Hum Hypertens *18*, 417-422.

Glancy, B., Kane, D.A., Kavazis, A.N., Goodwin, M.L., Willis, W.T., and Gladden, L.B. (2021). Mitochondrial lactate metabolism: history and implications for exercise and disease. J Physiol *599*, 863-888.

Gopal, K., Almutairi, M., Al Batran, R., Eaton, F., Gandhi, M., and Ussher, J.R. (2018). Cardiac-Specific Deletion of Pyruvate Dehydrogenase Impairs Glucose Oxidation Rates and Induces Diastolic Dysfunction. Front Cardiovasc Med *5*, 17.

Grujic, D., Susulic, V.S., Harper, M.E., Himms-Hagen, J., Cunningham, B.A., Corkey, B.E., and Lowell, B.B. (1997). Beta3-adrenergic receptors on white and brown adipocytes mediate beta3-selective agonist-induced effects on energy expenditure, insulin secretion, and food intake. A study using transgenic and gene knockout mice. J Biol Chem *272*, 17686-17693.

Harms, M., and Seale, P. (2013). Brown and beige fat: development, function and therapeutic potential. Nat Med *19*, 1252-1263.

Hattori, K., Naguro, I., Okabe, K., Funatsu, T., Furutani, S., Takeda, K., and Ichijo, H. (2016). ASK1 signalling regulates brown and beige adipocyte function. Nat Commun *7*, 11158.

Ikeda, K., Kang, Q., Yoneshiro, T., Camporez, J.P., Maki, H., Homma, M., Shinoda, K., Chen, Y., Lu, X., Maretich, P., et al. (2017). UCP1-independent signaling involving SERCA2b-mediated calcium cycling regulates beige fat thermogenesis and systemic glucose homeostasis. Nat Med *23*, 1454-1465.

Ikeda, K., Maretich, P., and Kajimura, S. (2018). The Common and Distinct Features of Brown and Beige Adipocytes. Trends Endocrinol Metab *29*, 191-200.

Inokuma, K., Okamatsu-Ogura, Y., Omachi, A., Matsushita, Y., Kimura, K., Yamashita, H., and Saito, M. (2006). Indispensable role of mitochondrial UCP1 for antiobesity effect of beta3-adrenergic stimulation. Am J Physiol Endocrinol Metab *290*, E1014-1021.

Ishibashi, J., and Seale, P. (2010). Medicine. Beige can be slimming. Science *328*, 1113-1114.

Kaisanlahti, A., and Glumoff, T. (2019). Browning of white fat: agents and implications for beige adipose tissue to type 2 diabetes. J Physiol Biochem *75*, 1-10.

Kajimura, S., and Saito, M. (2014). A new era in brown adipose tissue biology: molecular control of brown fat development and energy homeostasis. Annu Rev Physiol *76*, 225-249.

Kajimura, S., Spiegelman, B.M., and Seale, P. (2015). Brown and Beige Fat: Physiological Roles beyond Heat Generation. Cell Metab *22*, 546-559.

Kim, Y.J., Kim, H.J., Lee, S.G., Kim, D.H., In Jang, S., Go, H.S., Lee, W.J., and Seong, J.K. (2022). Aerobic exercise for eight weeks provides protective effects towards liver and cardiometabolic health and adipose tissue remodeling under metabolic stress for one week: A study in mice. Metabolism *130*, 155178.

Krauss, S., Zhang, C.Y., and Lowell, B.B. (2005). The mitochondrial uncoupling-protein homologues. Nat Rev Mol Cell Biol *6*, 248-261.

Lagarde, D., Jeanson, Y., Barreau, C., Moro, C., Peyriga, L., Cahoreau, E., Guissard, C., Arnaud, E., Galinier, A., Bouzier-Sore, A.K., et al. (2021). Lactate fluxes mediated by the monocarboxylate transporter-1 are key determinants of the metabolic activity of beige adipocytes. J Biol Chem *296*, 100137.

Langin, D. (2010). Adipose tissue lipolysis revisited (again!): lactate involvement in insulin antilipolytic action. Cell Metab *11*, 242-243.

Lee, D.K., Nguyen, T., Lynch, K.R., Cheng, R., Vanti, W.B., Arkhitko, O., Lewis, T., Evans, J.F., George, S.R., and O'Dowd, B.F. (2001). Discovery and mapping of ten novel G protein-coupled receptor genes. Gene *275*, 83-91.

Li, H., Hastings, M.H., Rhee, J., Trager, L.E., Roh, J.D., and Rosenzweig, A. (2020a). Targeting Age-Related Pathways in Heart Failure. Circ Res *126*, 533-551.

Li, Y., Ivica, N.A., Dong, T., Papageorgiou, D.P., He, Y., Brown, D.R., Kleyman, M., Hu, G., Chen, W.W., Sullivan, L.B., et al. (2020b). MFSD7C switches

mitochondrial ATP synthesis to thermogenesis in response to heme. Nat Commun *11*, 4837.

Luft, F.C. (2013). Finding a job for dichloroacetate. J Mol Med (Berl) *91*, 329-331.

Lye, M., and Donnellan, C. (2000). Heart disease in the elderly. Heart *84*, 560-566.

Miyamoto, S. (2019). Autophagy and cardiac aging. Cell Death Differ *26*, 653-664.

Moniotte, S., and Balligand, J.L. (2002). Potential use of beta(3)-adrenoceptor antagonists in heart failure therapy. Cardiovasc Drug Rev *20*, 19-26.

Mosterd, A., and Hoes, A.W. (2007). Clinical epidemiology of heart failure. Heart *93*, 1137-1146.

Okuno, D., Iino, R., and Noji, H. (2011). Rotation and structure of FoF1-ATP synthase. J Biochem *149*, 655-664.

Roland, C.L., Arumugam, T., Deng, D., Liu, S.H., Philip, B., Gomez, S., Burns, W.R., Ramachandran, V., Wang, H., Cruz-Monserrate, Z., and Logsdon, C.D. (2014). Cell surface lactate receptor GPR81 is crucial for cancer cell survival. Cancer Res *74*, 5301-5310.

Shuai, L., Zhang, L.N., Li, B.H., Tang, C.L., Wu, L.Y., Li, J., and Li, J.Y. (2019). SIRT5 Regulates Brown Adipocyte Differentiation and Browning of Subcutaneous White Adipose Tissue. Diabetes *68*, 1449-1461.

Tajima, K., Ikeda, K., Chang, H.Y., Chang, C.H., Yoneshiro, T., Oguri, Y., Jun, H., Wu, J., Ishihama, Y., and Kajimura, S. (2019). Mitochondrial lipoylation integrates age-associated decline in brown fat thermogenesis. Nat Metab *1*, 886-898.

Triposkiadis, F., Xanthopoulos, A., and Butler, J. (2019). Cardiovascular Aging and Heart Failure: JACC Review Topic of the Week. J Am Coll Cardiol *74*, 804-813.

Urbanska, K., and Orzechowski, A. (2019). Unappreciated Role of LDHA and LDHB to Control Apoptosis and Autophagy in Tumor Cells. Int J Mol Sci *20*.

Vaidya, A., Shakya, S., and Krettek, A. (2010). Obesity prevalence in Nepal: public health challenges in a low-income nation during an alarming worldwide trend. Int J Environ Res Public Health *7*, 2726-2744.

Vitali, A., Murano, I., Zingaretti, M.C., Frontini, A., Ricquier, D., and Cinti, S. (2012). The adipose organ of obesity-prone C57BL/6J mice is composed of mixed white and brown adipocytes. J Lipid Res *53*, 619-629.

Xiao, C., Goldgof, M., Gavrilova, O., and Reitman, M.L. (2015). Anti-obesity and metabolic efficacy of the beta3-adrenergic agonist, CL316243, in mice at thermoneutrality compared to 22 degrees C. Obesity (Silver Spring) *23*, 1450-1459.

Yao, Z., Yan, Y., Zheng, X., Wang, M., Zhang, H., Li, H., and Chen, W. (2020). Dietary Lactate Supplementation Protects against Obesity by Promoting Adipose Browning in Mice. J Agric Food Chem *68*, 14841-14849.

Zhang, J., Yang, J., Yang, N., Ma, J., Lu, D., Dong, Y., Liang, H., Liu, D., and Cang, M. (2020). Dlgap1 negatively regulates browning of white fat cells through effects on cell proliferation and apoptosis. Lipids Health Dis *19*, 39.

Zhang, Z., Yang, D., Xiang, J., Zhou, J., Cao, H., Che, Q., Bai, Y., Guo, J., and Su, Z. (2021). Non-shivering Thermogenesis Signalling Regulation and Potential Therapeutic Applications of Brown Adipose Tissue. Int J Biol Sci *17*, 2853-2870.

Zheng, J., and Ramirez, V.D. (2000). Inhibition of mitochondrial proton F0F1-ATPase/ATP synthase by polyphenolic phytochemicals. Br J Pharmacol *130*, 1115-1123.

Zhu, Y., Wu, J., and Yuan, S.Y. (2013). MCT1 and MCT4 expression during myocardial ischemic-reperfusion injury in the isolated rat heart. Cell Physiol Biochem *32*, 663-674.

국문 초록

# Lace1 유전자 결손마우스의

# 젖산 유도 베이지 지방 생성 연구

서울대학교 대학원

수의학과 수의생명과학 전공

(수의발생유전학)

김 연 주

(지도교수: 성 제 경)

백색 지방 조직의 갈변은 비만에 대한 에너지 항상성을 유지하는 데 필수적입니다. 최근 연구에 따르면 젖산 대사 산물은 β3-AR (β3-Adrenergic Receptor, 베타-3 아드레날린 수용체) 자극에 따라 백색 지방 조직(WAT) 갈변에 기여한다고 알려져 있습니다. Lace1 은 미토콘드리아 단백질 항상성을 매개하는 미토콘드리아 통합 막 단백질입니다. 그러나 이 유전자는 베이지 지방 조직에서의 역할은 알려져 있지 않습니다. 이 연구에서는 미토콘드리아 ATPase 유전자인 Lace1 이 심장에서 나오는 젖산염을 사용하여 CL-316,243(CL) 처리 시 백색 지방의 갈변 능력을 매개한다고 제안합니다.

베이지 지방에서 Lace1 발현을 조사하기 위해 베타 3 아드레날린 수용체(β3-ARs) 작용제인 CL 을 마우스에 3 일 동안 하루에 한 번 복강 주사 하였으며, 1 주일 동안 저온(4-6°C)에 노출시켰습니다. 또한, 마우스는 4 주 동안 자발적인 유산소 운동을 하며 훈련을 받았습니다. 갈색 및 베이지 지방세포에서 Lace1 의 기능을 확인하기 위해 C57BL/6N 마우스의 iBPA(immortalized brown pre-adipocyte, 갈색 전-지방 세포) 세포주와 기본 사타구니 백색 지방 세포를 사용했습니다. 또한 Lace1 유전자 결손(Knock-out, KO) 마우스에 CL 복강 주사, 저온 노출 및 자발적 유산소 운동을 적용하여 정상 마우스(Wild type, WT)와 비교하여 백색 지방의 갈변 능력, 갈색 지방의 활성화, 심장의 좌심실 비대를 확인했습니다.

Lace1 은 베이지 및 갈색 지방 생성 동안 증가했으며 백색 지방보다 CL, 저온 자극 및 운동 처리시, 정상 마우스에 비해 베이지 지방이

더 풍부했습니다. 저는 Lace1 과 Ucp1(uncoupling protein 1)이 갈변 자극 하에 백색 지방에서 양의 상관관계가 있다는 것을 발견했고, Lace1 유전자 결손 마우스는 CL 자극 및 저온 노출 시, 에너지 소비 증가와 함께 열 발생 관련 유전자 발현이 증가했음을 확인했습니다. 특히, Lace1 유전자 결손 마우스는 CL 자극 시 대조군에 비해 젖산 흡수 및 백색 지방의 갈변을 증가시켰습니다. Lace1 유전자 결손 마우스에서 젖산을 사용하여 향상된 갈변 능력은 심장 조직에서 피루브산 탈수소효소 (Pyruvate Dehydrogenase, PDH) 비활성화에 의한 젖산 방출 증가로 인한 것입니다.

이 연구는 심장으로부터 젖산 방출에 의해 백색지방의 갈변 능력을 매개하는 Lace1 의 역할을 확인하였습니다.

**주요어:** 레이스원, 베타-3 아드레날린 수용체, 저온 자극, 운동, 백색 지방, 베이지 지방, 갈색 지방, 백색 지방의 갈색화, 젖산염, 피루브산 탈수소효소

**학 번: 2015-21808**